2. Testad I, Aasland AM, Aarsland D. The effect of staff training on the use of restraint in dementia: a single-blind randomised controlled trial. *Int J Geriatr Psychiatry.* 2005;20:587-590.
3. Proctor R, Burns A, Powell HS, et al. Behavioural management in nursing and residential homes: a randomised controlled trial. *Lancet.* 1999;354:26-29.
4. Nakajima K. Qualifications and roles in the fields of elderly welfare and care. *Geriat Med.* 2005;43:1379-1388.
5. Kirpizidis H, Stavrati A, Geleris P. Assessment of quality of life in a randomized clinical trial of candesartan only or in combination with DASH diet for hypertensive patients. *J Cardiol.* 2005;46:177-182.
6. Ettema TP, Droes RM, de Lange J, et al. A review of quality of life instruments used in dementia. *Qual Life Res.* 2005;14:675-486.
7. Ballard CG, Margallo-Lana ML. The relationship between antipsychotic treatment and quality of life for patients with dementia living in residential and nursing home care facilities. *J Clin Psychiatry.* 2004;65(suppl 11):23-28.
8. Textbook Editorial Board, Tokyo Dementia Care Research and Training Center. *Practical Seminar on the Care of Demented Elderly People I and II.* Tokyo: Dai-ichi Hoki; 2002.
9. The Japanese Society for Dementia Care. *Dementia Care Textbook 1-4. Basics of Dementia Care.* Tokyo: World Planning; 2004.
10. Nakamura S. *Guideline for the Treatment of Patients With Dementia.* Tokyo: World Planning; 2003.
11. Terada S, Ishizu H, Fujisawa Y, et al. Development and evaluation of a health-related quality of life questionnaire for the elderly with dementia in Japan. *Int J Geriatr Psychiatry.* 2002;17:851-858.
12. Grossman M, Payer F, Onishi K, et al. Language comprehension and regional cerebral defects in frontotemporal degeneration and Alzheimer's disease. *Neurology.* 1998;50:157-163.
13. Pohjasvaara T, Erkinjuntti T, Ylikoski R, et al. Clinical determinants of poststroke dementia. *Stroke.* 1998;29:75-81.
14. Migneco O, Benoit M, Koulibaly PM, et al. Perfusion brain SPECT and statistical parametric mapping analysis indicate that apathy is a cingulate syndrome: a study in Alzheimer's disease and nondemented patients. *Neuroimage.* 2001;13:896-902.
15. Szirmai I, Vastagh I, Szombathelyi E, Kamondi A. Strategic infarcts of the thalamus in vascular dementia. *J Neurol Sci.* 2002;203-204:91-97.

Infection of Myeloid Dendritic Cells with *Listeria monocytogenes* Leads to the Suppression of T Cell Function by Multiple Inhibitory Mechanisms[1]

Alexey Popov,[2*] Julia Driesen,[2*] Zeinab Abdullah,[†] Claudia Wickenhauser,[‡] Marc Beyer,[*] Svenja Debey-Pascher,[*] Tomo Saric,[§] Silke Kummer,[‡] Osamu Takikawa,[¶] Eugen Domann,[‖] Trinad Chakraborty, Martin Krönke,[†] Olaf Utermöhlen,[†] and Joachim L. Schultze[3*]

Myeloid dendritic cells (DC) and macrophages play an important role in pathogen sensing and antimicrobial defense. In this study we provide evidence that myeloid DC respond to infection with *Listeria monocytogenes* with simultaneous induction of multiple stimulatory and inhibitory molecules. However, the overall impact of infected DC during T cell encounter results in suppression of T cell activation, indicating that inhibitory pathways functionally predominate. Inhibitory activity of infected DC is effected mainly by IL-10 and cyclooxygenase 2-mediated mechanisms, with soluble CD25 acting as an IL-2 scavenger as well as by the products of tryptophan catabolism. These inhibitory pathways are strictly TNF-dependent. In addition to direct infection, DC bearing this regulatory phenotype can be induced in vitro by a combination of signals including TNF, TLR2, and prostaglandin receptor ligation and by supernatants derived from the infected cells. Both infection-associated DC and other in vitro-induced regulatory DC are characterized by increased resistance to infection and enhanced bactericidal activity. Furthermore, myeloid DC expressing multiple regulatory molecules are identified in vivo in granuloma during listeriosis and tuberculosis. Based on the in vivo findings and the study of in vitro models, we propose that in granulomatous infections regulatory DC may possess dual function evolved to protect the host from disseminating infection via inhibition of granuloma destruction by T cells and control of pathogen spreading. *The Journal of Immunology*, **2008, 181: 4976–4988.**

Phagocytic cells play an important role in the defense against infectious pathogens including intracellular bacteria, for example, *Listeria monocytogenes* (*L.m.*)[4] (1) and *Mycobacterium tuberculosis* (2). Macrophages and neutrophils play a major role during early immune responses against these intracellular pathogens (3, 4), and yet, for a complete clearance of infection, an efficient adaptive immune response involving dendritic cells (DC) is required (1). As shown in listeriosis, DC are involved in pathogen elimination (5) and induction of Ag-specific $CD8^+$ T cell responses (6). In vitro studies demonstrated an induction of costimulatory molecules on human DC after *Listeria* infection (7, 8). However, there is also evidence that macrophages and DC infected by intracellular bacteria, viruses, and parasites can acquire regulatory phenotype and exert inhibitory function (9–12). Infection of human DC with *L.m.* leads to up-regulation of the immune inhibitory enzyme IDO, a key enzyme of tryptophan metabolism (10). Moreover, in vivo, an increase in DC numbers resulted in impaired protective immunity to subsequent infection of mice with *L.m.* (6), suggesting that DC-mediated inhibitory mechanisms might play a role in host-pathogen interaction.

During recent years, it has been suggested that DC are not only the most stimulatory cells for the induction of Ag-specific T cell responses (13), but that they are also capable of inhibiting T cell activation or even inducing T cell tolerance (14, 15). Numerous mechanisms have been linked to the phenotype of such cells, which are termed "tolerogenic" or "regulatory" DC (15–17). Down-regulation of costimulatory molecules (18) and stimulatory cytokines such as IL-12 (19), induction of coinhibitory molecules (e.g., PDL1 or TGF-β) (20, 21), as well as enzymatic mechanisms such as tryptophan catabolism (22, 23) have been identified as major inhibitory effectors of regulatory DC. The detrimental effect of such DC on Ag-specific immune responses is best illustrated in malignant disease (24), while their utility is explored in induction of tolerance in organ transplantation (15).

In infectious diseases, however, the existence of regulatory DC does not seem to be intuitively productive. We therefore examined regulation, expression, and function of immunoregulatory pathways in relation to granulomatous infection in vivo and in vitro primarily using *L.m.* and human DC as a model system. Under these conditions regulatory myeloid DC and macrophages seem to play a dual role within granuloma by impairing T cell-mediated

*Genomics and Immunoregulation, Institute for Life and Medical Sciences, University of Bonn, Bonn, Germany; †Institute for Medical Microbiology, Immunology and Hygiene, ‡Institute for Pathology, and §Institute for Neurophysiology, University of Cologne, Cologne, Germany; ¶National Institute for Longevity Sciences, National Center for Geriatrics and Gerontology, Obu, Aichi, Japan; and ‖Institute of Medical Microbiology, University of Giessen, Giessen, Germany

Received for publication March 28, 2008. Accepted for publication August 1, 2008.

The costs of publication of this article were defrayed in part by the payment of page charges. This article must therefore be hereby marked *advertisement* in accordance with 18 U.S.C. Section 1734 solely to indicate this fact.

[1] This work was supported by a Sofja Kovalevskaja Award from the Alexander von Humboldt Foundation (to J.L.S.), a Köln Fortune Grant (to J.L.S. and T.S.), grants of the Bundesministerium fuer Bildung and Forschung NGFN 01GS0111 (to T.C.) and NGFN N1K3-S24T27 (to J.L.S.) and grants from the Deutsche Forschungsgemeinschaft SFB704 (to J.L.S.), SFB589 (to C.W.), and SFB670 (to M.K. and O.U.).

[2] A.P. and J.D. contributed equally to this work.

[3] Address correspondence and reprint requests to Dr. Joachim L. Schultze, Laboratory for Genomics and Immunoregulation, Program Unit Molecular Immune and Cell Biology, LIMES (Life and Medical Sciences Bonn), University of Bonn, Karlrobert-Kreitenstrasse 13, D-53115 Bonn, Germany. E-mail address: j.schultze@uni-bonn.de

[4] Abbreviations used in this paper: *L.m.*, *Listeria monocytogenes*; COX-2, cyclooxygenase 2; DC, dendritic cells; DCreg, regulatory DC; immDC, immature DC; infDC, infected DC; matDC, mature DC; mo-DC, monocyte-derived DC; Pam_3, Pam_3Cys-Ser-$(Lys)_4$ trihydrochloride; PGE_2, prostaglandin E_2; PGE_2-DC, mature inhibitory DC stimulated with PGE_2; rhIL-2, recombinant human IL-2; sCD25, soluble CD25.

immune responses against the infected cells in the granuloma while at the same time inhibiting pathogen growth. Altogether, the induction of regulatory DC and macrophages especially in granulomatous infections might be favorable to the host.

Materials and Methods

Peripheral blood samples

Blood samples were collected from healthy blood donors at the Center for Transfusion Medicine after informed written consent was obtained. All experiments were approved by the University of Cologne Institutional Review Board.

Immunohistochemistry and immunofluorescence

Lymph node specimens from patients with clinically and serologically confirmed cervicoglandular listeriosis and tuberculosis were obtained from the Institute of Pathology (University of Cologne). As a control, tonsils and lymph nodes of uninfected patients were used. Immunohistochemical and immunofluorescence analyses of paraffin-embedded tissue samples were performed with Abs for S100, CD4, CD8, and CD83 (DakoCytomation), CD11c and CD25 (NovoCastra), CD56 (Zytomed), IDO (Serotec), cyclooxygenase 2 (COX-2) (IBL International), and FoxP3 (eBioscience) as described before (10).

Flow cytometry

Flow cytometry (FACSCanto, BD Biosciences) was performed using the following mAbs: CD3, CD11c, CD14, CD16, CD19, CD25, CD54, CD56, and anti-HLA-DR (BD Biosciences), CD11b, CD40, CD80, and CD86 (BD Pharmingen), anti-TNF-RI, anti-TNF-RII, and CCR7 (R&D Systems), CD58 and CD83 (Immunotech), and CD68 (Serotec) with appropriate isotype controls. Intracellular staining for IDO (monoclonal mouse anti-human IDO Ab) (25) and IFN-γ (IFN-γ-PE, Immunotech) was performed using Cytofix/Cytoperm Plus kit with GolgiStop (BD Biosciences) according to the manufacturer's instructions. All flow cytometric data were assessed with the BD CellQuest 3.3 software (BD Biosciences).

In vitro generation of monocyte-derived DC and macrophages

DC were generated according to standard protocols, as previously described (10, 26). For maturation, DC were incubated with TNF (Sigma-Aldrich), anti-CD40 mAb (BD Pharmingen) with or without prostaglandin E_2 (PGE_2, Sigma-Aldrich), as previously described (26). For some experiments, DC were treated with TNF in combination with PGE_2 and Pam_3Cys-Ser-$(Lys)_4$ trihydrochloride (Pam_3, Axxora, 1 μg/ml), TNF and PGE_2, TNF and Pam_3, or incubated with LPS (Sigma-Aldrich, 1 μg/ml). Alternatively, 50% of supernatants derived from immature DC (immDC), TNF-matured DC (matDC), or infected DC (infDC) were added to allogeneic immDC or matDC, respectively. Additionally, immDC were incubated with matDC or infDC in a 0.4-μm polycarbonate transwell system (Nunc). Macrophages were generated from monocytes, as previously described (10).

Infection of cells with L.m.

Wild-type strain (EGD) of *L.m.* was processed as previously described (10). Heat-killed *Listeria* were obtained by incubating wild-type bacteria at 65°C for 1 h. Monocytes, DC, and macrophages were infected with FITC-labeled *Listeria* or incubated with heat-killed *Listeria* at multiplicity of infection of 10 and infection efficiency was controlled by flow cytometry as previously described (10). Following the infection phase, cells were recultivated in fresh medium; for prolonged cultures (>12 h), gentamicin (50 μg/ml, Sigma-Aldrich) was added. For some experiments, DC treated with heat-killed *Listeria* were pulsed with recombinant human IL-2 (rhIL-2, Chiron) 24 h after the treatment onset and supernatants were collected after additional 48 h for functional assays.

Neutralization experiments

Listeria-infected DC were incubated with appropriate neutralizing mAbs or inhibitors, as previously described (10). The following Abs were used: anti-TNF mAb (20 μg/ml, BD Pharmingen), clinically applied TNF-neutralizing Ab infliximab (0.001–10 μg/ml, Centocor), anti-IFN-γ mAb (0.1–1 μg/ml, BD Pharmingen), anti-IL-10 mAb (5 μg/ml, R&D Systems), and anti-TNF-RI and anti-TNF-RII mAbs (10–100 μg/ml). The COX-2 inhibitor rofecoxib (a gift of Drs. K. Schrör and J. Meyer-Kirchrath) was used at 1–10 μM.

RNA preparation, microarray hybridization, and data processing

Immature DC were harvested on day 7 and mature DC were harvested 72 h upon start of maturation. Infected and corresponding control monocyte-derived DC (mo-DC) were harvested 2, 4, 6, and 24 h after infection. RNA and cRNA preparation, microarray hybridization (HG-U133A, Affymetrix), data analysis, and visualization were performed as previously described (10, 26). Microarray data are accessible at the National Center for Biotechnology Information (NCBI) Gene Expression Omnibus (GEO) database (accession no. GSE9946 at http://www.ncbi.nlm.nih.gov/geo/query/acc.cgi?acc).

Quantitative real-time PCR

Quantitative analysis of real-time PCR was performed using LightCycler3 and RelQuant software, version 1.0 (Roche Diagnostics), as previously described (10). Primers used (Roche Diagnostics) included: *IL2RA* forward, ACTGCTCACGTTCATCATGG, reverse, GATCTCTGGCGGGTC ATC, Universal ProbeLibrary probe no. 13; *B2M* forward, TTCTGGCC TGGAGGCTAT, reverse, TCAGGAAATTTGACTTTCCATTC, Universal ProbeLibrary probe no. 42.

Western blotting

COX-2 expression was assessed by anti-COX-2 polyclonal Ab (IBL International) as previously described (10). Alternatively, Western blots for COX-2 or IDO (25) were performed on the LI-COR Odyssey System (LI-COR Biosciences) according to the manufacturer's instructions.

ELISA

Soluble CD25, IL-2, TNF, IL-10, and IFN-γ in cell supernatants were measured by sIL-2R, IL-2, IFN-γ, IL-10, and TNF-α Eli-Pair kits (Diaclone Research) according to the manufacturer's instructions. All samples were analyzed at least in duplicates.

Assessment of kynurenine levels by photometrical assay

Assessment of kynurenine levels in the supernatants was performed as previously described (10, 25). Samples were run in triplicates against a standard curve of L-kynurenine concentrations (Sigma-Aldrich).

Mixed leukocyte reaction

MLR was performed as previously described (26). Briefly, freshly isolated allogeneic $CD4^+$ T cells were labeled with CFSE and incubated with DC at different ratios. DC were either incubated for 24 h in 96-well plates before T cells were added or they were additionally washed before MLR for the assay to be performed in fresh medium. In some experiments, magnetic beads, coated with anti-CD3 mAb or with anti-CD3 and anti-CD28 mAbs (27) at ratios of 1:1 or 1:10 (beads/T cells) were added. Alternatively, CD3/CD28-activated T cells were incubated with matDC or infDC in a transwell system. To neutralize the suppressive effect of infected DC, 1-methyl-tryptophan (10 μM, Sigma Aldrich), anti-IL-10 mAb (10 μg/ml), rofecoxib (10 μM), and rhIL-2 (20 U/ml) were given separately or in combination. After 3 days of culture, T cell proliferation was assessed by flow cytometry.

Inhibition of T cell proliferation

To study the effect of DC-derived soluble factors on CD3/CD28-induced T cell proliferation, CFSE-labeled $CD4^+$ T cells were incubated with L-kynurenine (Sigma-Aldrich), IL-10 (R&D Systems), or PGE_2 in a range of concentrations in either RPMI 1640 (Invitrogen) or in tryptophan-free RPMI 1640 medium (BioWhittaker) for 3 days until T cell proliferation was assessed by flow cytometry. Alternatively, CD3/CD28-activated T cells were incubated with supernatants derived from matDC or infDC (in a dilution range from 1 to 100%). In some experiments, T cell proliferation was assessed by incorporation of BrdU (Roche Diagnostics): cells were pulsed with BrdU on day 2 of culture and harvested 24 h thereafter; subsequently, BrdU incorporation was assessed according to the manufacturer's instructions.

Assessment of proliferation and viability of CTLL-2 cells

The murine IL-2-dependent T cell line CTLL-2 was obtained from the American Type Culture Collection (TIB-214) and cultured in supernatants derived from DC supplemented with rhIL-2 as previously described (26). Cell proliferation was determined by cell counting and viability assessed by flow cytometry with propidium iodide (Sigma-Aldrich).

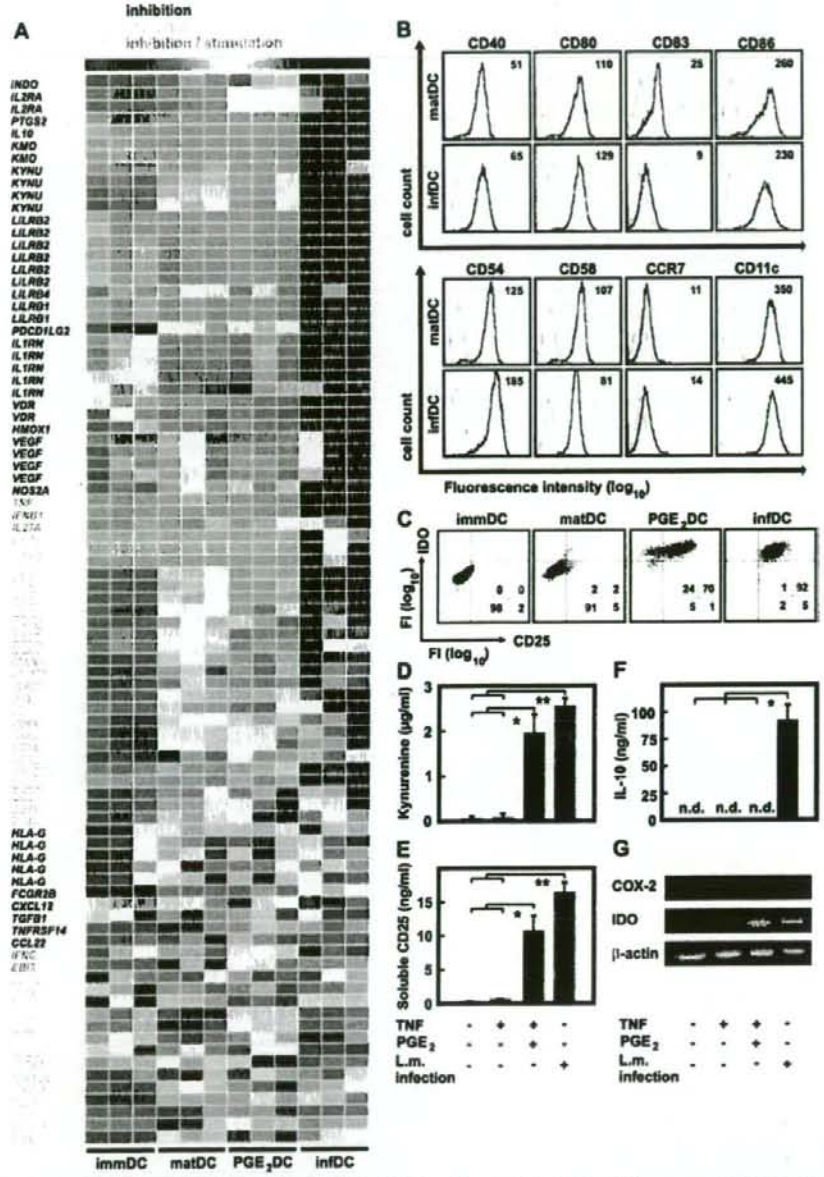

FIGURE 1. Induction of stimulatory and regulatory molecules during infection of human DC with *L.m.* DC were generated from monocytes as described in *Materials and Methods*. Asterisks highlight the statistically significant differences. *A*, Heat map displaying expression of genes associated with inhibitory or stimulatory function of DC. Average expression signals were obtained from microarray experiments and were standardized (*Z* score transformation) before visualization. Gene symbols for transcripts involved in stimulation or inhibition are differentially color-coded. Three independent DC cultures resulting in three array hybridizations were performed per DC subset and are shown in the heat map. *B*, Expression of activation markers, costimulatory molecules, and myeloid lineage marker CD11c by monocyte-derived DC either matured with TNF (matDC) or infected with *L.m.* (infDC) was studied by flow cytometry 24 h upon the start of maturation or infection, respectively. Isotype controls are shown as gray area underneath the thin line; expressionof specific Abs is reflected by thick black lines; mean fluorescence intensity values are shown in the right upper corner. One representative experiment of three is shown. *C*, Expression of CD25 (surface staining) and IDO (intracellular staining) by DC was assessed by flow cytometry (representative experiment, $n = 4$). Percentage of positive cells for each quadrant is shown in the right lower corner. *D*, Kynurenine accumulation in supernatants as a measure of IDO activity was assessed using a photometric assay (mean + SD, $n = 4$). *, $p < 0.005$ and **, $p < 0.00005$. *E*, Secretion of soluble CD25 was assessed by ELISA (mean ± SD, $n = 4$). *, $p < 0.005$ and **, $p < 0.0005$. *F*, IL-10 secretion was assessed by ELISA (mean ± SD, $n = 4$). *, $p < 0.005$; n.d., not detectable. *G*, Protein expression of COX-2 and β-actin (as loading control) was assessed by Western blot. After stripping, the membrane was additionally incubated with IDO mAb. One representative experiment out of four is shown.

Assessment of L.m. *viability*

Immediately after infection, DC were lysed and the number of viable *Listeria* (initial bacterial burden) was determined in a CFU assay on blood agar. Consequently, bactericidal activity of DC was analyzed after various periods of time. Additionally, *L.m.* was incubated for 6 h in a tryptophan-free RPMI 1640 medium supplemented with different concentrations of L-tryptophan and L-kynurenine (Sigma Aldrich) and *Listeria* viability was controlled by CFU assay.

Statistical analysis

Statistical analysis was performed using R software package (version 2.3.0). To calculate statistical significance, a two-sample two-tailed *t* test was used. Comparisons with a *p*-value <0.05 were called statistically significant.

Results

Human DC express numerous stimulatory and inhibitory molecules upon infection with L.m.

We have recently demonstrated that infection of human DC with *L.m.* leads to the induction of the immunoinhibitory enzyme IDO (10), while in other studies *L.m.* infection was associated with a stimulatory DC phenotype (7, 8). To clarify this apparent discrepancy we performed detailed comparative microarray analysis on myeloid DC infected with *L.m.* (infDC) (10), mature inhibitory DC stimulated with prostaglandin E_2 (PGE_2-DC) and expressing IDO (26), mature stimulatory DC lacking the expression of IDO (matDC), and immDC. For presentation of differentially expressed transcripts associated with inhibitory or stimulatory DC function (reviewed in detail in Refs. 16, 17) expression values were standardized using Z score transformation at the probeset level and visualized as a heat map.

As shown in Fig. 1*A*, infDC are enriched for numerous transcripts associated with stimulatory as well as inhibitory DC function. Among inhibitory genes *PTGS2* (COX-2), *IL10* (IL-10), and *IL2RA* (CD25), enzymes of tryptophan catabolism and inhibitory Ig-like transcripts were most strongly induced in infDC (Fig. 1*A*). Furthermore, transcripts for TNF, IFN-β, and IL-23, which can exert antiinflammatory action (28), were up-regulated only in infDC. Stimulatory genes induced by infection included various chemokines, cell adhesion (*ICAM1* and *CD58*) and costimulatory molecules (*CD40*, *CD80*, *CD86*, and *TNFSF9*). However, other important stimulatory molecules, such as *CD83*, *CCR7*, *CCL19*, TNF superfamily members, and CD1 family molecules were only up-regulated in noninfected stimulatory matDC (Fig. 1*A*). Altogether, infDC present a rather specific transcriptional "signature" that distinguishes them from immDC, stimulatory matDC, and inhibitory PGE_2-DC: they simultaneously express numerous inhibitory as well as stimulatory molecules.

Assessment of surface receptor expression by flow cytometry demonstrated that infDC and stimulatory matDC expressed comparable amounts of costimulatory and adhesion molecules but differed in expression of CD83 (Fig. 1*B*). To corroborate transcriptional regulation of inhibitory molecules, expression of CD25, IL-10, and COX-2 was assessed using IDO as a control marker for regulatory DC (17). Cell-surface CD25 is up-regulated in virtually all infDC and is coexpressed with intracellular IDO, while only 70% of inhibitory PGE_2-DC expressed CD25 (Fig. 1*C*). ImmDC and matDC did not express CD25 and IDO. Supernatants from infDC contained significant amounts of kynurenine as a consequence of functional IDO expression (Fig. 1*D*). Moreover, infDC secreted large amounts of soluble CD25 (sCD25) (Fig. 1*E*). The onset of CD25 mRNA expression, as assessed by quantitative real-time PCR, was faster and the amount of secreted sCD25 after *L.m.* infection was higher (data not shown) as compared with PGE_2-DC (30). In contrast to CD25 and IDO, IL-10 and COX-2 were only induced by infDC but not by other DC subsets (Fig. 1, *F* and *G*). The kinetics of IL-10 secretion resembled that of sCD25 (data not shown). Altogether, infection of myeloid DC by *L.m.* induces stimulatory molecules together with numerous inhibitory pathways previously associated with regulatory DC function (16, 17).

Functional predominance of inhibitory pathways in infected DC

In light of expression of inhibitory and stimulatory molecules by infDC, we next studied the impact of infDC on T cell activation. First, the stimulatory capacity of infDC in comparison to other DC subsets was assessed in an allogeneic MLR using purified $CD4^+$ T cells and beads coated with low-dose anti-CD3 mAb, thus providing equal signal 1 for all conditions (27). Treatment of T cells with anti-CD3 beads alone did not induce T cell proliferation or T cell cytokine production (Fig. 2*A* and data not shown). Co-cultures of T cells and matDC in the presence of anti-CD3 beads induced significant T cell proliferation (Fig. 2*A*) comparable to beads coated with anti-CD3 and anti-CD28 Abs (Fig. 2*A*). However, when T cells were cocultured with DC without anti-CD3 beads, proliferation was very low (Fig. 2*A*), and therefore the following MLR experiments were performed with anti-CD3 coincubation.

To study the effect of infection on DC stimulatory capacity, matDC and infDC were simultaneously coincubated with allogeneic CFSE-labeled $CD4^+$ T cells in the presence of anti-CD3 beads, and after 3 days T cell proliferation was assessed by flow cytometry. Significant reduction in T cell proliferation (up to 60%) was observed when T cells were coincubated with infDC, pointing out that infDC display an impaired ability to stimulate $CD4^+$ T cells compared with matDC (Fig. 2*B*). Reduced T cell proliferation was accompanied by reduced IFN-γ production (data not shown). In the second set of experiments, DC were preincubated for 24 h (to allow induction of inhibitory mechanisms after infection) and prior T cells were added for a coculture (Fig. 2*C*). Under these conditions T cell proliferation was also significantly reduced (up to 75%) in the presence of infDC (Fig. 2*C*), and this reduction was even more profound as in a direct coculture (Fig. 2*B*).

Subsequently, we determined whether infected DC can suppress the proliferation of activated T cells when provided with a strong stimulatory signal (anti-CD3 plus anti-CD28 beads). For this purpose, DC were added to T cell/bead cocultures at the onset of stimulation (Fig. 2*D*). T cells strongly proliferated when stimulated by anti-CD3/anti-CD28 beads, and addition of matDC did not significantly increase T cell proliferation (Fig. 2*D*). In contrast, proliferation of CD3/CD28-activated T cells was significantly lower when cocultured with infected DC (Fig. 2*D*). The suppression of CD3/CD28-induced T cell proliferation was even more evident when the stimulus was suboptimal (1:10 ratio of beads/T cells, Fig. 2*D*). Interestingly, when this assay was performed in a transwell system, where DC were separated from T cell/bead cocultures by a 0.4-μm polycarbonate membrane, the difference between matDC and infDC was substantially less prominent (~10%, data not shown).

Timing of interaction between DC and T cells has an impact on T cell activation (29). Therefore, in the next set of experiments we studied whether pretreatment of T cells with a stimulatory signal (anti-CD3/anti-CD28 beads) for 24 h prior to MLR would have an impact on the suppressive effect of infDC (Fig. 2*E*). In contrast to the experiments presented in Fig. 2*D*, addition of infDC to prestimulated T cells did not alter the proliferation rate of the latter, even when the CD3/CD28 stimulus was suboptimal (Fig. 2*E*). These data indicate that infDC cannot exert inhibitory effects upon previously activated T cells. Altogether, the outcome of encounter between T cells and infDC depends on the timing and T cell preactivation status.

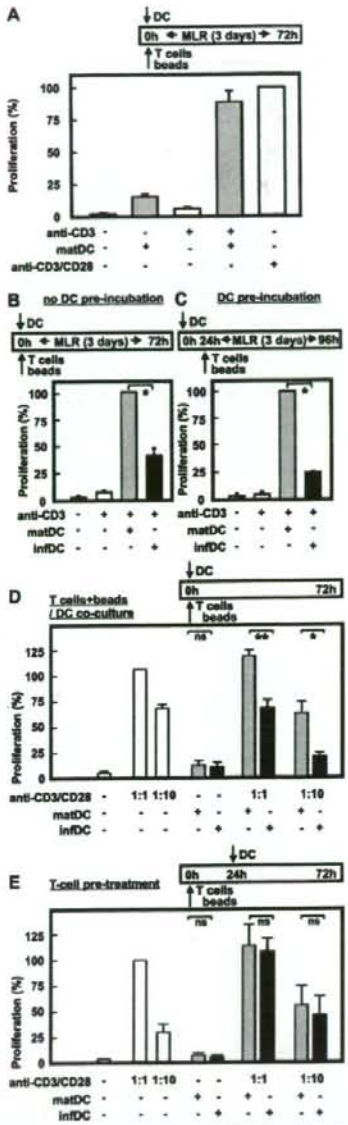

FIGURE 2. DC infected with *L.m.* inhibit T cell proliferation. Immature DC were either infected with *L.m.* (infDC) or stimulated with TNF (matDC). Allogeneic CFSE-labeled $CD4^+$ T cells were coincubated with DC at a ratio of 10:1 (T cells to DC), and beads, coated with either anti-CD3 mAb (anti-CD3) or anti-CD3 and anti-CD28 mAbs (anti-CD3/CD28), were added at different ratios. Asterisks highlight the statistically significant differences; ns, not significant. *A*, Mature DC were cocultured with T cells and anti-CD3 or anti-CD3/CD28 beads (beads/T cell ratio 1:1). After 3 days of coculture, T cell proliferation was assessed by flow cytometry. In the diagram, percentages of proliferating T cells of three independent experiments (relative to the simulation with anti-CD3/CD28 beads alone, taken as 100%; mean ± SD) are shown. *B*, Mature DC or infected DC were extensively washed and cocultured with T cells and anti-CD3 beads without preincubation (beads/T cell ratio 1:1). After 3 days of coculture T cell proliferation was assessed by flow cytometry. Percentages of proliferating T cells of three independent experiments (relative to the simulation with matDC, taken as 100%; mean ± SD) are shown. *, $p < 0.005$. *C*, Mature DC or infected DC were preincubated at 1×10^5/ml in 96-well plates. After 24 h, T cells and anti-CD3 beads were added (beads/T cell ratio 1:1), and after further 3 days of culture T cell proliferation was assessed by flow cytometry. Percentages of proliferating T cells of three independent experiments (relative to the simulation with matDC, taken as 100%; mean ± SD) are shown. *, $p < 0.0001$. *D*, Allogeneic CFSE-labeled $CD4^+$ T cells were coincubated with anti-CD3 and anti-CD28 beads (beads/T cells ratio 1:1 for optimal simulation and 1:10 for suboptimal stimulation; light gray bars). Simultaneously, mature DC stimulated with TNF (matDC, dark gray bars) or DC infected with *L.m.* (infDC, black bars) were added to T cells at a ratio of 1:10 (DC/T cells). As a control, T cells were left unstimulated or stimulated with DC alone. Three days upon the onset of T cell culture, T cell proliferation was assessed by flow cytometry. In the diagram, percentages of proliferating T cells of three independent experiments (relative to the optimal simulation with anti-CD3/CD28 beads (ratio 1:1) alone, taken as 100%; mean ± SD) are shown. *, $p < 0.05$ and **, $p < 0.005$. *E*, Same as *D*, except that DC were added only 24 h after the onset of T cell/beads coculture.

Next we assessed whether infDC-derived soluble factors are sufficient to suppress the CD3/CD28-activated T cell proliferation (Fig. 3). For this purpose, CD3/CD28-activated T cells were incubated with a concentration range of DC-derived supernatants (0–100%) or with kynurenine, IL-10, and PGE_2; the latter assay was also performed in a tryptophan-free medium. Addition of infDC-derived supernatants to activated T cells resulted in a significant suppression of T cell proliferation, starting from 20% dilution, when compared with the same amount of matDC-derived supernatants (Fig. 3*A*).

Furthermore, addition of kynurenine to CD3/CD28-activated T cells was sufficient to suppress the T cell proliferation, and this effect was even more profound when the assay was performed in a tryptophan-free medium (Fig. 3*B*). Combination of low tryptophan and kynurenine (as a model of IDO enzymatic activity), as well as addition of IL-10 or PGE_2, led to a comparable and significant reduction of CD3/CD28-induced T cell proliferation (Fig. 3*B*).

While inhibitory functions of IL-10 (30), IDO (14), and COX-2-mediated PGE_2 (27) have been well established (Fig. 3*B*), the role of cell-surface CD25 and soluble CD25 is less clear (26, 31). IL-2-dependent CTLL-2 cells and heat-killed *L.m.* were used to address this question. Heat-killed *L.m.* induce similar amounts of CD25 in infDC (data not shown) but no IDO and COX-2 (10), so it was chosen to study the function of CD25 expression on infected DC. As shown in Fig. 3*C*, the number of viable CTLL-2 cells was significantly reduced in cultures incubated with supernatants from infDC in comparison to matDC. As a consequence, an increase of dead CTLL-2 cells in supernatants from infDC was observed (Fig. 3*D*). This was associated with a 30% reduction of IL-2 in culture supernatants as measured by ELISA (data not shown).

To determine the impact of individual inhibitory mechanisms, $CD4^+$ T cells were cocultured with infDC together with IL-2 (as a CD25 antagonist) and inhibitors against COX-2, IL-10, or IDO. Blockade of IDO, COX-2, and IL-10 individually did not significantly change T cell proliferation in presence of infDC, and IL-2 was also without effect (Fig. 3*E*). Only with inhibiting COX-2, IL-10, and IDO in the presence of IL-2 was an increase in T cell proliferation detected (Fig. 3*E*). Overall, these data indicate that multiple inhibitory mechanisms that are capable to turn infDC into regulatory DC are induced during infection.

Regulatory phenotype of infected DC is controlled predominantly by TNF

In addition to IFNs (14), we have recently revealed TNF as a potent inducer of the inhibitory molecule IDO (10). Here, we assessed the role of IFN-γ, TNF, and TNF-RI and TNF-RII on the

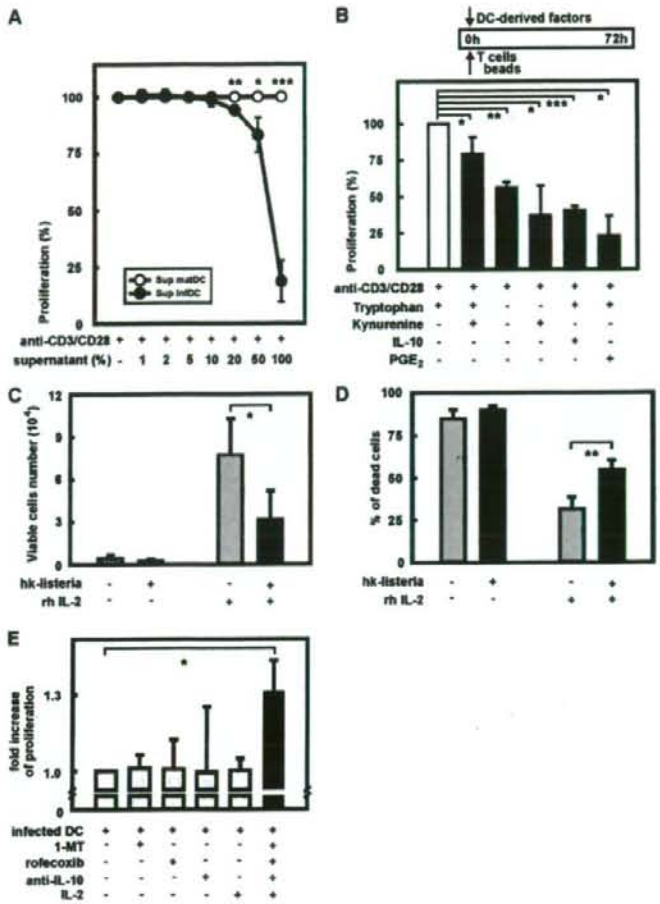

FIGURE 3. Multiple inhibitory pathways must be blocked in infected DC to rescue T cell proliferation. *A*, CFSE-labeled $CD4^+$ T cells were coincubated with anti-CD3 and anti-CD28 beads (beads/T cells ratio 1:1) in CellGro medium supplemented with supernatants, derived from matDC (○) or infDC (●) (in a dilution range from 1 to 100%). In the diagram, percentages of T cells proliferating in infDC-derived supernatants (●) are shown relative to T cells cultured in matDC-derived supernatants (○), taken as 100% (mean ± SD; $n = 4$). *, $p < 0.05$; **, $p < 0.005$; and ***, $p < 0.001$. *B*, $CD4^+$ T cells were coincubated with anti-CD3 and anti-CD28 beads (beads/T cells ratio 1:1) in tryptophan-containing RPMI 1640 medium either alone (white bar) or together with L-kynurenine (5 μg/ml), IL-10 (100 ng/ml), or PGE_2 (1 μg/ml) (black bars). Alternatively, tryptophan-free RPMI 1640 medium with or without L-kynurenine was used. Three days upon the onset of T cell culture, T cell proliferation was assessed by flow cytometry (CFSE) or measuring BrdU incorporation. In the diagram, percentages of proliferating T cells of three independent experiments (relative to the simulation with anti-CD3/CD28 beads (ratio 1:1) in tryptophan-containing RPMI 1640 (white bar), taken as 100%; mean ± SD) are shown. *, $p < 0.05$; **, $p < 0.005$; and ***, $p < 0.001$. *C* and *D*, Analysis of cell proliferation (*C*) and viability (*D*) of the IL-2-dependent cell line CTLL-2. Supernatants from $CD25^+$ DC incubated with heat-killed *L.m.* (hk-listeria, black bars) or from $CD25^-$ nontreated DC (gray bars) were supplemented with rhIL-2 and added to CTLL-2 cells. CTLL-2 cell viability and cell numbers were assessed after 48 h (mean ± SD, $n = 4$). *, $p < 0.05$ and **, $p < 0.005$. *E*, To neutralize the suppressive effect of infected DC, IDO inhibitor 1-methyl-tryptophan (10 μM, Sigma-Aldrich), anti-IL-10 mAb (10 μg/ml), COX-2 inhibitor rofecoxib (10 μM), and rhIL-2 (20 U/ml) were added to the MLR at the time of onset separately or in combination. Increase of T cell proliferation is shown relative to T cell cultures in the presence of infected DC (mean ± SD, $n = 3$). *, $p < 0.05$.

induction of the IDO-associated inhibitory molecules CD25, IL-10, and COX-2 during DC infection. TNF-RI and TNF-RII are expressed in infDC (data not shown), while TNF and IFN-γ are secreted by infected DC with TNF production preceding IFN-γ production (10). Secreted TNF was completely sequestered by anti-TNF mAb (infliximab) and was not blocked by Abs against TNF receptors (anti-TNF-RI, anti-TNF-RII) or IFN-γ (Fig. 4*A*). In contrast, IFN-γ was significantly reduced by neutralization of TNF or blocking of TNF-RI/RII, indicating that IFN-γ acts downstream of TNF receptor signaling in infDC (Fig. 4*B*). To control the experiments addressing regulation of CD25, IL-10, and COX-2, we assessed IDO and kynurenine induction. Blockade of TNF or IFN-γ significantly reduced IDO expression and abrogated kynurenine production and this was mediated by both TNF-RI and TNF-RII signaling (Fig. 4, *C* and *D*). Expression of cell-surface and particularly of soluble CD25 was similarly reduced by the blockade of TNF and TNF-RI/II signaling (Fig. 4, *E* and *F*). However, in contrast to IDO, blockade of IFN-γ did not alter expression of CD25 and secretion of sCD25. This was similarly true for IL-10 secretion (Fig. 4*G*) and COX-2 protein induction (Fig. 4*H*), which were inhibited by blockade of TNF but not by IFN-γ. Dose dependency of TNF-mediated induction of CD25, IL-10, COX-2, and also IDO was demonstrated by increasing doses of infliximab or anti-TNF-R Abs (data not shown). Inhibition of IL-10 or COX-2 did not alter expression of CD25 or IDO (data not shown). Altogether, this places TNF as a central mediator of inhibitory molecules in DC during *L.m.* infection. TNF receptor-mediated signaling is required for induction of IFN-γ, COX-2, IL-10, CD25, and IDO, whereas IFN-γ is only necessary for IDO induction.

Regulatory DC suppress the growth of L.m.

Based on up-regulation of molecules involved in tryptophan metabolism (IDO, KMO, KYNU; see Fig. 1*A*), we postulated that tryptophan reduction might play a role in defense against *L.m.* (32). To assess *Listeria* uptake and bactericidal capacity, we first searched for an appropriate model system. The models were defined by a comparison of comprehensive transcriptional signatures of infected DC, described herein, and of differentially treated DC performed by ourselves or derived from publicly accessible databases, and by a regulatory DC (DCreg) phenotype, which we defined to be CD25/IDO/COX-2 and IL-10. Treatment of immDC with a combination of TNF and Pam_3, as well as with TNF, PGE_2, and Pam_3 (A. Popov, unpublished observations) or LPS (33) (data accessible at NCBI GEO database, accession no. GSE2706, at link provided above) resulted in up-regulation of *IL2RA*, *INDO*, *IL10*, and *PTGS2* as well as genes coding for bactericidal peptides, toxic oxygen, and nitrogen radicals' donors and acidic proteases (data not shown). Moreover, TNF/

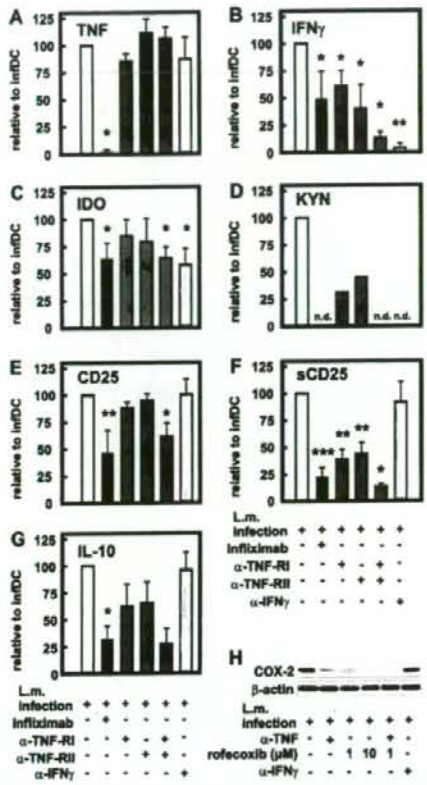

FIGURE 4. Induction of DC with regulatory phenotype is controlled by TNF. Immature DC were infected with wild-type *L.m.* Immediately after infection, DC were incubated with anti-TNF Ab infliximab (1 μg/ml, black bars), anti-TNF-RI (α-TNF-RI), or anti-TNF-RII (α-TNF-RII) mAbs (100 μg/ml, dark gray bars) or anti-IFN-γ mAb (α-IFN-γ, 1 μg/ml, light gray bars). Cells and supernatants were harvested 24 h postinfection. Percentage of reduction was calculated relative to the values derived from DC, infected by wild-type *Listeria*, taken as 100% (white bar). Asterisks highlight the statistically significant comparisons of various treatments vs *Listeria*-infected untreated DC. *A*, Secretion of TNF was measured by ELISA (mean ± SD; at least three independent experiments were performed). *, $p < 0.000005$. *B*, Secretion of IFN-γ was measured by ELISA (mean ± SD; at least three independent experiments were performed). *, $p < 0.05$ and **, $p < 0.00005$. *C*, IDO expression was assessed by flow cytometry as shown in Fig. 1*B* and mean fluorescence intensity values were compared (mean ± SD, $n = 3$). *, $p < 0.05$. *D*, Kynurenine (KYN) accumulation was assessed using a photometric assay. n.d., not detectable. *E*, Analysis of cell-surface expression of CD25 was performed by flow cytometry (mean ± SD; at least three independent experiments were performed). *, $p < 0.05$ and **, $p < 0.005$. *F*, Analysis of sCD25 concentration was performed by ELISA (mean ± SD; at least three independent experiments were performed). *, $p < 0.05$; **, $p < 0.005$; and ***, $p < 0.00005$. *G*, Secretion of IL-10 was measured by ELISA (mean ± SD; $n = 3$ except for combination of anti-TNF-R ($n = 2$)). *, $p < 0.01$. *H*, Protein expression of COX-2 and β-actin (as loading control) was assessed by Western blot. Infected DC were either left untreated or were treated with anti-TNF mAb (α-TNF, 20 μg/ml), COX-2 inhibitor rofecoxib (1–10 μM), or anti-IFN-γ mAb (α-IFN-γ, 1 μg/ml). One representative experiment out of five is shown.

PGE_2/Pam_3 and LPS treatment resulted in the induction of a DCreg phenotype (Fig. 5*A*). To address if a comparable phenotype can be induced in human DC, which are associated with infection foci but are not infected themselves, we incubated immDC or matDC with the supernatants derived from the allogeneic immDC, matDC, or infDC, respectively. All supernatants were double sterile filtered (0.2 μm) and seeded on agar plates to assure the absence of bacteria before the experiment (data not shown). As shown in Fig. 5*B*, incubation of immDC with infDC-derived supernatants, but not with the supernatants derived from immDC or matDC, resulted in the induction of the DCreg phenotype. Comparable results were obtained in a transwell system when immDC (lower chamber) were cocultured with infDC (upper chamber) and when mature DC were treated with the supernatants derived from infected DC (data not shown).

For additional experiments we mostly used TNF/PGE_2/Pam_3-induced DC as a model for IDO^+ DCreg. Different DC subsets (immDC, matDC, DCreg) were infected with FITC-labeled *L.m.* at a multiplicity of infection of 10 and bacterial burden was analyzed over time after infection. As determined by uptake of bacteria, susceptibility to infection with *L.m.* differed between various DC populations (Fig. 5*C*). As expected, immDC were more easily infected than IDO^- matDC and IDO^+ DCreg. Among the latter two, IDO^+ DCreg were most resistant against infection and phagocytosed less *Listeria* than did matDC. Within the first 30 min after infection, all DC subsets substantially reduced the initial bacterial load; however, on a cell-to-cell basis, IDO^+ DCreg were significantly more efficient in controlling the phagocytosed *Listeria* than IDO^- immDC or IDO^- matDC (Fig. 5*D*, relative number of intracellular viable bacteria derived 30 min after infection and normalized to the initial time point ($t = 0$) set to 100% is shown). Moreover, only IDO^+ DCreg were able to significantly restrict the number of viable intracellular bacteria over time, while the number of viable *L.m* in matDC and immDC significantly increased during the course of infection (Fig. 5*E*). Importantly, DC expressing a regulatory phenotype were equally efficient in "managing" intracellular *Listeria* independently of the factors used for inducing the DCreg phenotype, such as TNF/PGE_2/Pam_3, TNF/Pam_3, LPS, or supernatant-treated DCreg (Fig. 5*E* and data not shown). In contrast, immature DC and DC matured with TNF or anti-CD40 appeared to lose the control over the intracellular bacteria (Fig. 5*E* and data not shown). Overall, fewer IDO^+ DCreg are infected by *L.m.* and those infected are more sufficient in reducing and controlling bacterial load, independently of the agents that induce the regulatory phenotype.

To assess the effect of IDO-mediated tryptophan catabolism on *L.m.*, the survival of *L.m.* was determined in vitro under different concentrations of tryptophan and one of its key downstream metabolites, kynurenine. Growth of *L.m.* was influenced both by tryptophan starvation and toxic metabolites (as exemplified for kynurenine), with kynurenine being more potent than tryptophan reduction in suppressing bacterial growth (Fig. 5*F*).

Regulatory phenotype hallmarks DC in human chronic listeriosis in vivo

To address the in vivo relevance of our findings, we examined CD25 and COX-2 expression in lymph node specimens of patients with serologically confirmed cervicoglandular-type listeriosis with suppurative granuloma. These granulomas consist mostly of $S100^+CD11c^+$ DC and, to a lesser extent, of $CD68^+CD11c^+$ macrophages (10). In fact, most of the cells forming the outer border of the granuloma expressed the DC marker S100 and substantial amounts of IDO, CD25, and also COX-2 (Fig. 6*A*). Of note, granuloma-forming DC did not express the DC activation marker CD83 (Fig. 6*A*), supporting the transcriptional data and the

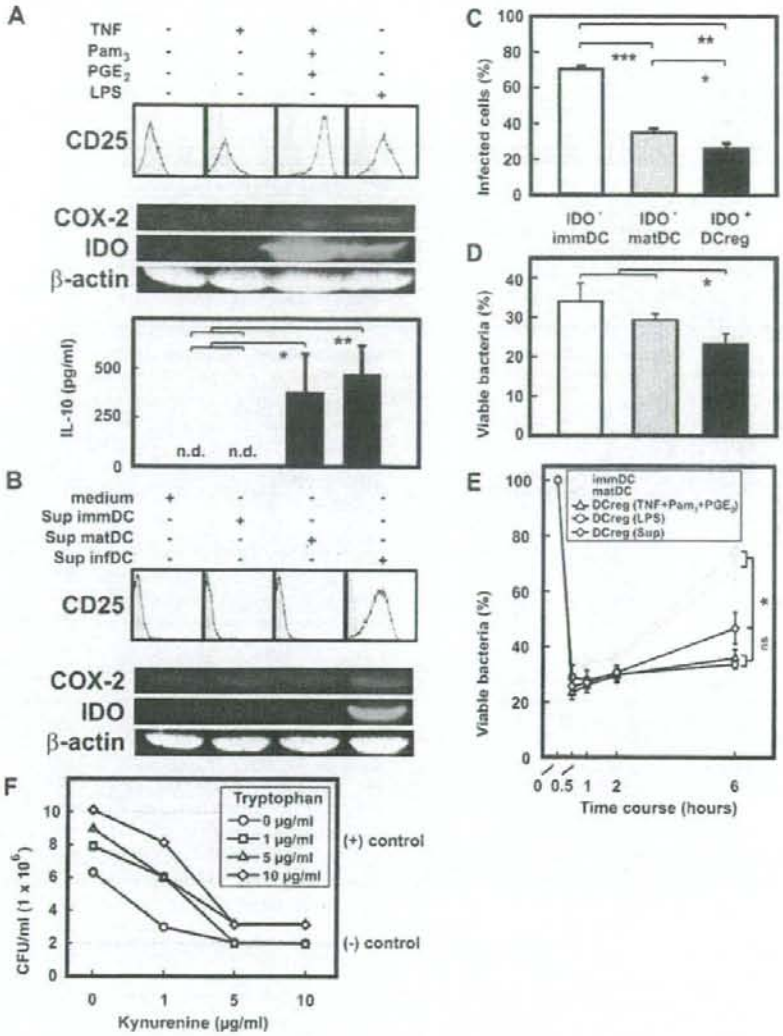

FIGURE 5. Susceptibility of various DC populations for infection with *L.m.* DC were generated from monocytes as described in *Materials and Methods*. IDO$^-$ immDC indicates immature DC; IDO$^-$ matDC, DC matured with TNF; IDO$^+$ DCreg, DC stimulated with either combination of TNF, PGE_2, and Pam_3. LPS, or supernatants derived from infected DC (Sup). Asterisks highlight the statistically significant comparisons; ns indicates not significant. *A* and *B*, Expression of surface CD25 (flow cytometry) or COX-2 and IDO proteins (Western blot) was assessed in immature DC treated for 3 days with either (*A*) TNF, TNF + PGE_2 + Pam_3, or LPS or (*B*) supernatants derived from immDC, matDC, or infDC (50%). ImmDC, treated with medium alone, and TNF-matured DC were used as controls. Representative experiments are shown; at least four independent experiments were performed per condition. In the lower part of *A*, IL-10 secretion by differentially treated DC assessed by ELISA is shown (mean ± SD, $n = 3$). *, $p < 0.05$; **, $p < 0.01$; and n.d., not detectable. *C*, Infection rates of IDO$^-$ immDC (white bar), IDO$^-$ matDC (gray bar), and IDO$^+$ DCreg (TNF + PGE_2 + Pam_3, black bar) by FITC-labeled *L.m.* were assessed by flow cytometry after the extracellular bacteria were removed (mean ± SD, $n = 3$). *, $p < 0.05$; **, $p < 0.0005$; and ***, $p < 0.0001$. *D*, Bactericidal activity of IDO$^-$ immDC (white bar), IDO$^-$ matDC (gray bar), and IDO$^+$ DCreg (TNF + PGE_2 + Pam_3, black bar) infected with *L.m.* was assessed in a CFU assay 30 min after infection. Graph represents the relative number of intracellular viable bacteria derived from DC 30 min after infection (normalized to the initial time point ($t = 0$) set to 100%; mean ± SD, $n = 3$). *, $p < 0.05$. *E*, Bactericidal activity of human DC infected with *L.m.* was assessed over time in a CFU assay. Graph represents kinetics of intracellular viable bacteria at specified time points normalized to the initial time point ($t = 0$) set to 100% (mean ± SD, $n = 3$). *, $p < 0.01$ (between DCreg treated with intDC-derived supernatants and either IDO$^-$ immDC or IDO$^-$ matDC). *F*, *L.m.* was incubated in a tryptophan-free RPMI 1640 medium supplemented with L-tryptophan and L-kynurenine (0–10 μg/ml), and after 6 h the number of *Listeria* was determined as CFU. Negative control, HBSS buffer; positive control, RPMI 1640 medium with tryptophan. Representative experiment with similar results from three independent cultures performed on 3 different days is shown.

results of cell-surface staining (see Fig. 1*B*). Morphological assessment, as well as FoxP3 staining, excluded a massive infiltration of CD25$^+$ regulatory T cells; however, some FoxP3$^+$ cells were present within the granuloma wall and more FoxP3$^+$ cells were detected between the granuloma (Fig. 6*A*). Staining with mAbs specific for CD4, CD8, and CD56 demonstrated that T cells

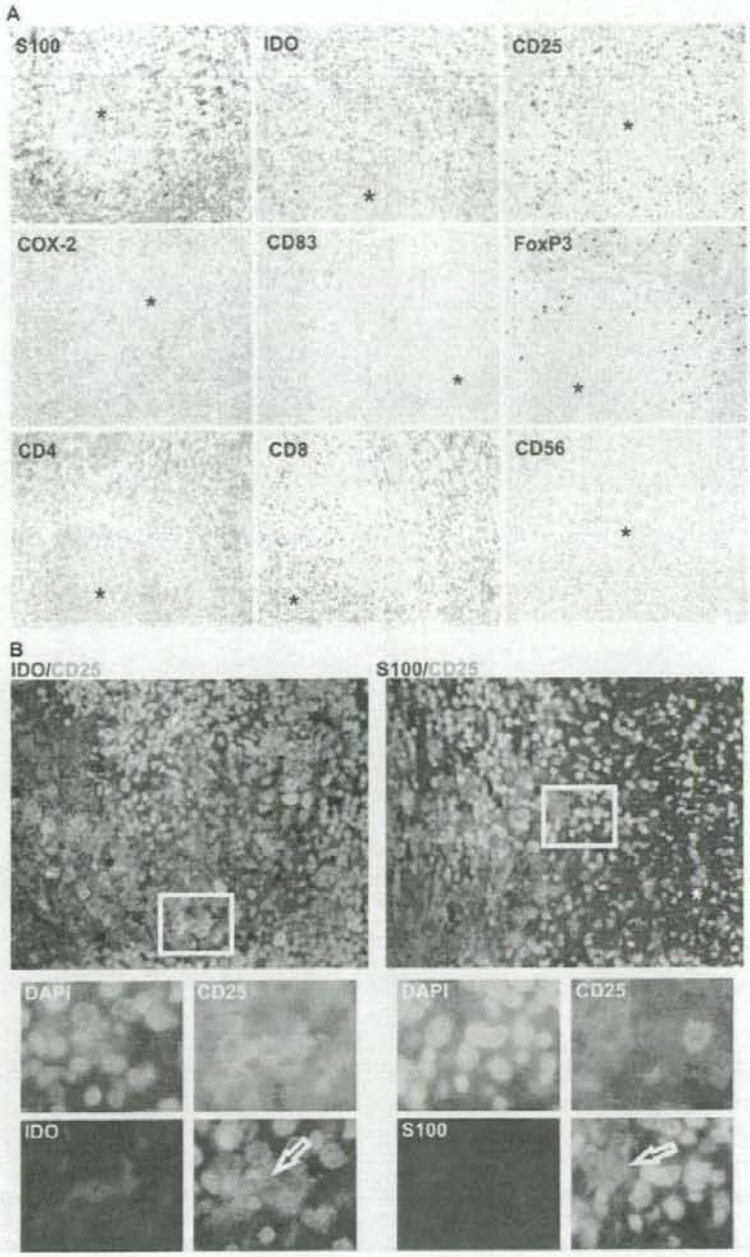

FIGURE 6. DC with regulatory phenotype form the granuloma wall in advanced human listeriosis. Histomorphology of lymph node sections from a patient with cervicoglandular-type suppurative granulomatous listeriosis. One representative case out of three is shown. Asterisks point out the center of granuloma. *A*, Immunohistochemistry of listerial granuloma. Outer ringwall of granuloma in advanced human listeriosis consists of DC (S100). A great majority of cells forming the ringwall around granuloma express IDO and CD25 and stain positive for COX-2, whereas no $CD83^-$ cells are revealed within granuloma ringwall and around granuloma. Single $FoxP3^+$ cells are located within the granuloma wall and outside of the granuloma. $CD4^+$ and $CD8^+$ T cells are located around the granuloma (outside of the ringwall); no $CD56^+$ NK cells are found in the rim or around the granuloma. Magnification, ×250. *B*, Double immmunofluorescence staining for IDO (red, cytoplasmatic staining) and CD25 (green, membrane staining) reveal $CD25^+IDO^+$ cells in granuloma ringwall; magnification, ×400. Double immmunofluorescence staining for S100 (red, cytoplasmatic staining) and CD25 (green) reveal $CD25^+$ DC in granuloma ringwall; magnification, ×400. *Below*, an enlarged section of each photo (marked with a white rectangle; magnification, ×1000) is shown for more detail for every staining separately (DAPI, CD25, and either IDO or S100) and in overlay; double-positive cells (either IDO^+CD25^+ or $CD25^+S100^+$) are highlighted with white arrows.

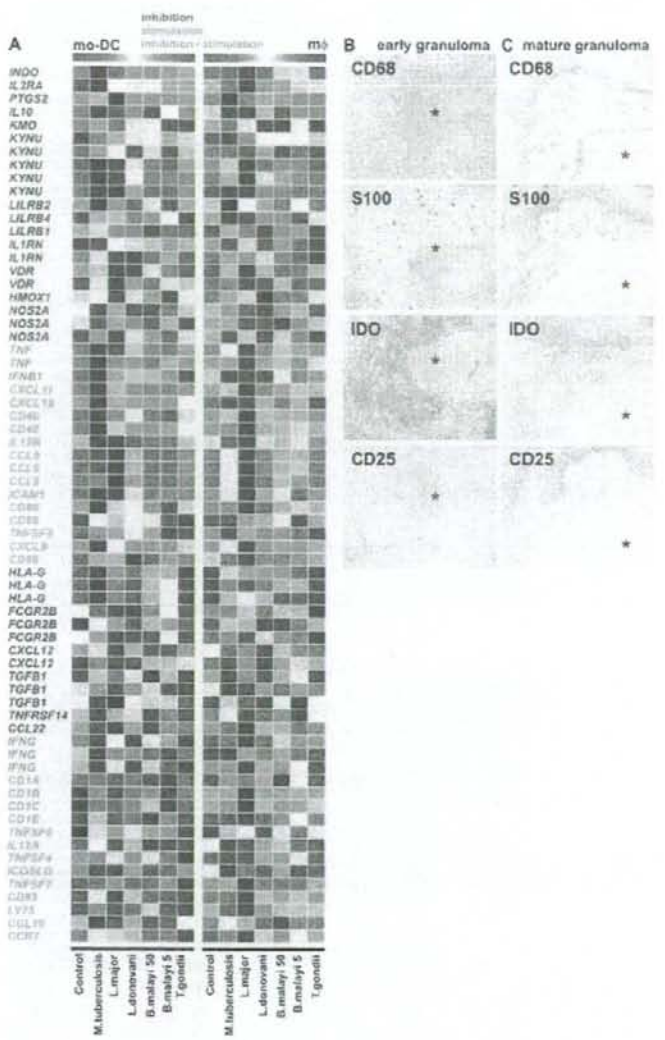

FIGURE 7. Myeloid cells with regulatory phenotype are induced in granuloma during tuberculosis. *A*, Heat map displaying average expression signals of inhibitory and stimulatory genes (Fig. 1*A*). Expression values for mo-DC and macrophages (Mϕ) infected with phylogenetically distinct parasites and bacteria were obtained from NCBI GEO (accession no. GSE360 at http://www.ncbi.nlm.nih.gov/projects/geo/) and average expression signals were standardized (Z score transformation) before visualization. Due to use of a different microarray platform (HG-U95A) several transcripts assessed in Fig. 1*A* (*PDCD1LG2*, *IL23A*, *HMOX1*, *VEGF*, *EBI3*) were not imprinted on the chip and therefore were excluded from the analysis. Transcripts involved in stimulation or inhibition are differentially color-coded. *B*, Immunohistochemistry of early stage granuloma in tuberculosis (*M. tuberculosis*); images of macrophage marker CD68, DC marker S100, IDO, and CD25 were taken at magnification of ×100. Asterisks point out the center of granuloma. One representative experiment of three is shown. *C*, Immunohistochemistry of late-stage mature granuloma (same legend as in *B*).

were displaced in the area between the granuloma, whereas NK cells were almost absent. Although we did not perform the costaining of FoxP3 and CD4, based on the spatial localization of both markers, FoxP3$^+$ cells might be regulatory T cells. Using two-color immunofluorescence analysis, we demonstrated that CD25 and IDO are coexpressed by S100$^+$ DC (Fig. 6*B*). Double staining for CD11c and CD25 confirmed CD25$^+$ DC to be of myeloid origin (data not shown). CD68$^+$ macrophages within the granuloma ringwall also expressed CD25, but to a lesser extent as DC (data not shown). Macrophages generated from monocytes and infected with *L.m.* expressed surface CD25, secreted sCD25, and expressed COX-2, albeit to a lesser extent than infDC (data not shown). Altogether, myeloid DC and macrophages within the granuloma express multiple inhibitory molecules associated with a regulatory phenotype of DC (15).

Induction of regulatory DC in other granulomatous infections

If formation and maintenance of granuloma rely on inhibitory pathways induced in myeloid cells, we hypothesized that other pathogens associated with granuloma formation would induce comparable molecular programs. To address this question, we applied the transcriptional signature of stimulatory and inhibitory genes established for *L.m.* infection (see Fig. 1*A*) to a publicly available dataset describing the genome-wide response of human DC and macrophages to phylogenetically distinct pathogens (data accessible at NCBI GEO database, accession no. GSE360, at link provided above) (34). Infection of DC with *M. tuberculosis* and macrophages with *Leishmania major* most closely resembled the expression pattern observed for *L.m.* infection. Induction of transcripts for TNF, IFN-γ, CD25, COX-2, IL-10, and enzymes of the tryptophan catabolism (IDO, KMO, KYNU) was apparent in DC infected with either of these three pathogens (Fig. 7*A*). Similarly, genes encoding stimulatory molecules (e.g., *CD40*, *CD80*, *CD86*, *ICAM1*, and *CD58*) induced in human DC by *L.m.* infection were also induced by *M. tuberculosis* and *L. major*. Other infections assessed in this experiment (Fig. 7*A*) clearly differed in the regulation of stimulatory and inhibitory pathways. To assess the in vivo relevance of these findings, we assessed expression of IDO, CD25,

and COX-2, as well as DC marker S100 and macrophage marker CD68, in granuloma in tuberculosis. The structure of tubercular granuloma is regulated within time: as the granuloma matures, collagen-rich fibers substitute the cells at the periphery, which leads to granuloma organization (35). To determine whether expression of regulatory proteins by granuloma-forming cells is also regulated over time, we examined their expression in the early as well as late-stage granuloma. In contrast to listeriosis, $CD68^+$ macrophages were the major cellular component of early granuloma in tuberculosis, while only few $S100^+$ DC were present; expression of IDO was very prominent and CD25 was moderately expressed (Fig. 7*B*), whereas COX-2 staining was rather faint (data not shown). Costaining experiments revealed that $CD25^+$ cells do express IDO as well as CD11c, confirming their myeloid origin (data not shown). However, regulatory cells seem to be an early event during granuloma formation, since $CD25^+$ IDO^+ cells were almost absent in late-stage granuloma, although macrophages and DC were still present (Fig. 7*C*).

Discussion

Tryptophan-catabolizing DC are a major component of granuloma in human listeriosis (10). Herein we demonstrate that granuloma-forming myeloid cells, either DC or macrophages, in human listeriosis and tuberculosis are characterized by coinduction of multiple inhibitory pathways, including CD25 secretion, IL-10 expression, COX-2-dependent mechanisms, as well as tryptophan catabolism. Using listeriosis as a model we linked the induction of this regulatory phenotype of myeloid DC to infection and established TNF as the major mediator of inhibitory proteins, while IFN-γ, which is downstream of TNF, is only required for induction of the tryptophan-catabolizing enzyme IDO. Regulatory DC induced during infection with *L.m.* are strong inhibitors of T cell activation, and their regulatory function can be reversed only by simultaneous blockade of several inhibitory proteins. The modest recovery of T cell proliferation when blocking four regulatory proteins at once (Fig. 3*E*) underscores the predominance of the regulatory DC phenotype over the stimulatory one and points out that even more regulatory mechanisms might be involved (Fig. 1*A*). Regulatory DC are not only endowed with the ability to suppress T cell function, but also to suppress bacterial infection. While tryptophan metabolism in regulatory DC seems to play an important role in reducing bacterial burden during infection, other unknown factors must account for the increased resistance of regulatory DC to infection. Altogether, these findings advocate that regulatory myeloid cells involved in granuloma formation during listeriosis and tuberculosis are provided with multiple inhibitory mechanisms evolved to protect the host from disseminating infection while at the same time inhibiting granuloma destruction by T cells.

Accumulating data suggest that DC, in addition to macrophages, play an important role in the pathogenesis of granulomatous diseases such as listeriosis, tuberculosis, or cat-scratch disease (4, 10, 36, 37). Infection of DC with various pathogens was associated with induction of stimulatory effects on DC function by these pathogens or their components (7, 8, 38). We corroborate these data, demonstrating that important stimulatory molecules (e.g., CD40, CD80, and CD86) are induced in DC and macrophages during infection with *L.m.* and *M. tuberculosis* (Figs. 1 and 7). However, simultaneous induction of several inhibitory pathways (IL-10, COX-2, CD25, and IDO) does counterbalance these stimulatory pathways toward inhibition of T cell function. Furthermore, IL-10 was reported to inhibit pathogen-specific T cell responses (39), and prostaglandins, products of COX-2-mediated arachidonic acid metabolism, were shown to suppress cellular immunity to *Listeria* (40). At the same time both factors directly suppress T cell proliferation (27, 30) and are also involved in the induction of regulatory T cells (41, 42). For CD25, we demonstrated that cell-surface and soluble CD25 induced by infection can function as an IL-2 scavenger receptor. This is in line with clinical evidence linking increased levels of sCD25 to immunosuppression in infectious (43–45) and malignant diseases (46, 47). Of note, induction of CD25 and sCD25, as well as IDO, is not restricted to mo-DC, but has been observed in $BDCA\text{-}1^+$ primary myeloid DC stimulated ex vivo with lipoteichoic acid derived from *L.m.* (A. Popov, unpublished observation) or with PGE_2 (26).

The balance between the stimulatory and inhibitory phenotype of regulatory DC does not result only from the expression of stimulatory or inhibitory molecules, but also from the kinetics of interaction with $CD4^+$ T cells as well as the activation status of the T cells. If the inhibitory phenotype of regulatory DC is elicited before encounter of T cells, their suppressive effect will be clearly more pronounced. Conversely, preactivation of T cells via TCR and costimulatory signals can neutralize the inhibitory effect of regulatory DC.

The bactericidal effect of tryptophan depletion in different cells expressing the key enzymes of the tryptophan pathway has been recognized for several pathogens (32). For *L.m.*, conflicting data concerning the role of tryptophan metabolism have been reported. Although *L.m.* was shown to be auxotrophic for tryptophan (48), growth of the virulent strains of *Listeria* is regarded to be tryptophan independent (49) due to expression of tryptophan synthase genes (*trp*) enabling autonomous tryptophan production (50). Herein we demonstrate that IDO^+ DC are most effective in reducing bacterial burden and infection. Moreover, bacterial growth appears to be predominantly regulated by the accumulation of its toxic metabolite kynurenine. A lower sensitivity to tryptophan starvation compared with the effect of toxic metabolites is in line with previous findings (50). Gram-positive bacteria can produce tryptophan autonomously, making them insensitive to fluctuations in tryptophan concentration in the environment but still vulnerable to the accumulation of toxic metabolites (50). However, IDO^- DC were capable of initially reducing bacterial burden postinfection, suggesting that other mechanisms are utilized by regulatory DC during pathogen containment. Altogether, these data emphasize the importance of tryptophan metabolism for regulatory DC function; however, both T cell suppression as well as pathogen inhibition rely on a multitude of inhibitory mechanisms acting in concert.

An intriguing finding was the hierarchy of signals necessary to induce inhibitory molecules after *Listeria* infection. Clearly, TNF is a main mediator inducing CD25, COX-2, IL-10, and IDO in DC. Furthermore, both TNF receptors are essential for TNF signaling since both had to be blocked to achieve maximum reduction of inhibitory proteins. Most striking, however, was the finding that IFN-γ is clearly downstream of TNF signaling and only governs induction of IDO but not the other inhibitory pathways. The major function of granulomatous structures is the containment of pathogens that otherwise cannot be eradicated by the immune system, thereby preventing an uncontrolled systemic spreading of the pathogen (51, 52). TNF has been recognized as an important factor governing formation and maintenance of granuloma containing intracellular pathogens such as *M. tuberculosis* or *L.m.* (53, 54). However, strict TNF dependency of multiple important inhibitory mechanisms in regulatory DC came somewhat as a surprise since this might be the granuloma's Achilles' heel. Clinical evidence is in line with our experimental data. In patients with rheumatoid arthritis elevated sCD25 serum levels are significantly reduced after treatment with the TNF-neutralizing drug infliximab (55). Suppression of IDO and IL-10 during infliximab therapy was recently

reported for patients with Crohn's disease (56, 57). More dramatic, a severe side effect of anti-TNF therapy is in fact exacerbation of granulomatous listeriosis or tuberculosis mediated by T cells destroying the granulomas (58, 59).

Collectively, this study provides strong evidence that intracellular pathogens such as *M. tuberculosis* and *L.m.* induce a specific transcriptional program in myeloid DC and macrophages characterized by a functional preponderance of multiple inhibitory mechanisms. On the one hand, these myeloid regulatory cells are equipped to suppress unwanted T cell attacks against granulomatous structures; on the other hand, they prohibit pathogens from spreading throughout the host. The exact mechanisms, however, should be studied in the proper animal models. Of particular interest for further research will be the exploitation of the yet unknown pathways of myeloid regulatory cells conferring resistance to infection. This might lead to the discovery of novel strategies protecting other cells from overwhelming infection with these devastating intracellular pathogens.

Acknowledgments

We thank our colleagues from the Center for Transfusion Medicine for providing us with peripheral blood products, and we are grateful to all blood donors. We thank Mirela Stecki and Julia Claasen for technical assistance. We are in debt to Dr. Alexander Poyarkov for his invaluable help during the study design and manuscript preparation. We also thank Drs. K. Schrör and J. Meyer-Kirchrath from the Institute for Pharmacology and Clinical Pharmacology, University of Düsseldorf, Germany, for providing rofecoxib, and Daniela Eggle for critical reading of the manuscript.

Disclosures

The authors have no financial conflicts of interest.

References

1. Pamer, E. G. 2004. Immune responses to *Listeria monocytogenes*. *Nat. Rev. Immunol.* 4: 812–823.
2. Flynn, J. L., and J. Chan. 2001. Immunology of tuberculosis. *Annu. Rev. Immunol.* 19: 93–129.
3. Grivennikov, S. I., A. V. Tumanov, D. J. Liepinsh, A. A. Kruglov, B. I. Marakusha, A. N. Shakhov, T. Murakami, L. N. Drutskaya, I. Forster, B. E. Clausen, et al. 2005. Distinct and nonredundant in vivo functions of TNF produced by T cells and macrophages/neutrophils: protective and deleterious effects. *Immunity* 22: 93–104.
4. Tsai, M. C., S. Chakravarty, G. Zhu, J. Xu, K. Tanaka, C. Koch, J. Tufariello, J. Flynn, and J. Chan. 2006. Characterization of the tuberculous granuloma in murine and human lungs: cellular composition and relative tissue oxygen tension. *Cell Microbiol.* 8: 218–232.
5. Serbina, N. V., T. P. Salazar-Mather, C. A. Biron, W. A. Kuziel, and E. G. Pamer. 2003. TNF/iNOS-producing dendritic cells mediate innate immune defense against bacterial infection. *Immunity* 19: 59–70.
6. Alaniz, R. C., S. Sandall, E. K. Thomas, and C. B. Wilson. 2004. Increased dendritic cell numbers impair protective immunity to intracellular bacteria despite augmenting antigen-specific $CD8^+$ T lymphocyte responses. *J. Immunol.* 172: 3725–3735.
7. Kolb-Maurer, A., I. Gentschev, H. W. Fries, F. Fiedler, E. B. Brocker, E. Kampgen, and W. Goebel. 2000. *Listeria monocytogenes*-infected human dendritic cells: uptake and host cell response. *Infect. Immun.* 68: 3680–3688.
8. Paschen, A., K. E. Dittmar, R. Grenningloh, M. Rohde, D. Schadendorf, E. Domann, T. Chakraborty, and S. Weiss. 2000. Human dendritic cells infected by *Listeria monocytogenes*: induction of maturation, requirements for phagolysosomal escape and antigen presentation capacity. *Eur. J. Immunol.* 30: 3447–3456.
9. de Graaff, P. M., E. C. de Jong, T. M. van Capel, M. E. van Dijk, P. J. Roholl, J. Boes, W. Luytjes, J. L. Kimpen, and G. M. van Bleek. 2005. Respiratory syncytial virus infection of monocyte-derived dendritic cells decreases their capacity to activate CD4 T cells. *J. Immunol.* 175: 5904–5911.
10. Popov, A., Z. Abdullah, C. Wickenhauser, T. Saric, J. Driesen, F. G. Hanisch, E. Domann, E. L. Raven, O. Dehus, C. Hermann, et al. 2006. Indoleamine 2,3-dioxygenase-expressing dendritic cells form suppurative granulomas following *Listeria monocytogenes* infection. *J. Clin. Invest.* 116: 3160–3170.
11. Poncini, C. V., C. D. Alba Soto, E. Batalla, M. E. Solana, and S. M. Gonzalez Cappa. 2008. *Trypanosoma cruzi* induces regulatory dendritic cells in vitro. *Infect. Immun.* 76: 2633–2641.
12. Wong, K. A., and A. Rodriguez. 2008. *Plasmodium* infection and endotoxic shock induce the expansion of regulatory dendritic cells. *J. Immunol.* 180: 716–726.
13. Banchereau, J., and R. M. Steinman. 1998. Dendritic cells and the control of immunity. *Nature* 392: 245–252.
14. Munn, D. H., M. D. Sharma, J. R. Lee, K. G. Jhaver, T. S. Johnson, D. B. Keskin, B. Marshall, P. Chandler, S. J. Antonia, R. Burgess, et al. 2002. Potential regulatory function of human dendritic cells expressing indoleamine 2,3-dioxygenase. *Science* 297: 1867–1870.
15. Morelli, A. E., and A. W. Thomson. 2007. Tolerogenic dendritic cells and the quest for transplant tolerance. *Nat. Rev. Immunol.* 7: 610–621.
16. Steinman, R. M., D. Hawiger, and M. C. Nussenzweig. 2003. Tolerogenic dendritic cells. *Annu. Rev. Immunol.* 21: 685–711.
17. Popov, A., and J. L. Schultze. 2008. IDO-expressing regulatory dendritic cells in cancer and chronic infection. *J. Mol. Med.* 86: 145–160.
18. Jonuleit, H., E. Schmitt, G. Schuler, J. Knop, and A. H. Enk. 2000. Induction of interleukin 10-producing, nonproliferating $CD4^+$ T cells with regulatory properties by repetitive stimulation with allogeneic immature human dendritic cells. *J. Exp. Med.* 192: 1213–1222.
19. Kalinski, P., C. M. Hilkens, A. Snijders, F. G. Snijdewint, and M. L. Kapsenberg. 1997. IL-12-deficient dendritic cells, generated in the presence of prostaglandin E_2, promote type 2 cytokine production in maturing human naive T helper cells. *J. Immunol.* 159: 28–35.
20. Selenko-Gebauer, N., O. Majdic, A. Szekeres, G. Hofler, E. Guthann, U. Korthauer, G. Zlabinger, P. Steinberger, W. F. Pickl, H. Stockinger, et al. 2003. B7-H1 (programmed death-1 ligand) on dendritic cells is involved in the induction and maintenance of T cell anergy. *J. Immunol.* 170: 3637–3644.
21. Ghiringhelli, F., P. E. Puig, S. Roux, A. Parcellier, E. Schmitt, E. Solary, G. Kroemer, F. Martin, B. Chauffert, and L. Zitvogel. 2005. Tumor cells convert immature myeloid dendritic cells into TGF-β-secreting cells inducing $CD4^+$ $CD25^+$ regulatory T cell proliferation. *J. Exp. Med.* 202: 919–929.
22. Munn, D. H., and A. L. Mellor. 2007. Indoleamine 2,3-dioxygenase and tumor-induced tolerance. *J. Clin. Invest.* 117: 1147–1154.
23. Puccetti, P., and U. Grohmann. 2007. IDO and regulatory T cells: a role for reverse signalling and non-canonical NF-κB activation. *Nat. Rev. Immunol.* 7: 817–823.
24. Sharma, M. D., B. Baban, P. Chandler, D. Y. Hou, N. Singh, H. Yagita, M. Azuma, B. R. Blazar, A. L. Mellor, and D. H. Munn. 2007. Plasmacytoid dendritic cells from mouse tumor-draining lymph nodes directly activate mature Tregs via indoleamine 2,3-dioxygenase. *J. Clin. Invest.* 117: 2570–2582.
25. Takikawa, O., T. Kuroiwa, F. Yamazaki, and R. Kido. 1988. Mechanism of interferon-gamma action. Characterization of indoleamine 2,3-dioxygenase in cultured human cells induced by interferon-gamma and evaluation of the enzyme-mediated tryptophan degradation in its anticellular activity. *J. Biol. Chem.* 263: 2041–2048.
26. von Bergwelt-Baildon, M. S., A. Popov, T. Saric, J. Chemnitz, S. Classen, M. S. Stoffel, F. Fiore, U. Roth, M. Beyer, S. Debey, et al. 2006. CD25 and indoleamine 2,3-dioxygenase are up-regulated by prostaglandin E_2 and expressed by tumor-associated dendritic cells in vivo: additional mechanisms of T-cell inhibition. *Blood* 108: 228–237.
27. Chemnitz, J. M., J. Driesen, S. Classen, J. L. Riley, S. Debey, M. Beyer, A. Popov, T. Zander, and J. L. Schultze. 2006. Prostaglandin E_2 impairs $CD4^+$ T cell activation by inhibition of lck: implications in Hodgkin's lymphoma. *Cancer Res.* 66: 1114–1122.
28. Zakharova, M., and H. K. Ziegler. 2005. Paradoxical anti-inflammatory actions of TNF-α: inhibition of IL-12 and IL-23 via TNF receptor 1 in macrophages and dendritic cells. *J. Immunol.* 175: 5024–5033.
29. Iezzi, G., K. Karjalainen, and A. Lanzavecchia. 1998. The duration of antigenic stimulation determines the fate of naive and effector T cells. *Immunity* 8: 89–95.
30. Groux, H., M. Bigler, J. E. de Vries, and M. G. Roncarolo. 1996. Interleukin-10 induces a long-term antigen-specific anergic state in human $CD4^+$ T cells. *J. Exp. Med.* 184: 19–29.
31. Velten, F. W., F. Rambow, P. Metharom, and S. Goerdt. 2007. Enhanced T-cell activation and T-cell-dependent IL-2 production by $CD83^+$, $CD25^{bright}$, $CD43^{bright}$ human monocyte-derived dendritic cells. *Mol. Immunol.* 44: 1555–1561.
32. MacKenzie, C. R., K. Heseler, A. Muller, and W. Daubener. 2007. Role of indoleamine 2,3-dioxygenase in antimicrobial defence and immuno-regulation: tryptophan depletion versus production of toxic kynurenines. *Curr. Drug Metab.* 8: 237–244.
33. Napolitani, G., A. Rinaldi, F. Bertoni, F. Sallusto, and A. Lanzavecchia. 2005. Selected Toll-like receptor agonist combinations synergistically trigger a T helper type 1-polarizing program in dendritic cells. *Nat. Immunol.* 6: 769–776.
34. Chaussabel, D., R. T. Semnani, M. A. McDowell, D. Sacks, A. Sher, and T. B. Nutman. 2003. Unique gene expression profiles of human macrophages and dendritic cells to phylogenetically distinct parasites. *Blood* 102: 672–681.
35. Cosma, C. L., D. R. Sherman, and L. Ramakrishnan. 2003. The secret lives of the pathogenic mycobacteria. *Annu. Rev. Microbiol.* 57: 641–676.
36. Uchira, K., R. Amakawa, T. Ito, K. Tajima, S. Naitoh, Y. Ozaki, T. Shimizu, K. Yamaguchi, Y. Uemura, H. Kitajima, et al. 2002. Dendritic cells are decreased in blood and accumulated in granuloma in tuberculosis. *Clin. Immunol.* 105: 296–303.
37. Vermi, W., F. Facchetti, E. Riboldi, H. Heine, S. Scutera, S. Stornello, D. Ravarino, P. Cappello, M. Giovarelli, R. Badolato, et al. 2006. Role of dendritic cell-derived CXCL13 in the pathogenesis of *Bartonella henselae* B-rich granuloma. *Blood* 107: 454–462.
38. Hertz, C. J., S. M. Kiertscher, P. J. Godowski, D. A. Bouis, M. V. Norgard, M. D. Roth, and R. L. Modlin. 2001. Microbial lipopeptides stimulate dendritic cell maturation via Toll-like receptor 2. *J. Immunol.* 166: 2444–2450.
39. Biswas, P. S., V. Pedicord, A. Ploss, E. Menet, I. Leiner, and E. G. Pamer. 2007. Pathogen-specific CD8 T cell responses are directly inhibited by IL-10. *J. Immunol.* 179: 4520–4528.

40. Petit, J. C., G. Richard, B. Burghoffer, and G. L. Daguet. 1985. Suppression of cellular immunity to *Listeria monocytogenes* by activated macrophages: mediation by prostaglandins. *Infect. Immun.* 49: 383–388.
41. Levings, M. K., S. Gregori, E. Tresoldi, S. Cazzaniga, C. Bonini, and M. G. Roncarolo. 2005. Differentiation of Tr1 cells by immature dendritic cells requires IL-10 but not CD25$^+$ CD4$^+$ Tr cells. *Blood* 105: 1162–1169.
42. Sharma, S., S. C. Yang, L. Zhu, K. Reckamp, B. Gardner, F. Baratelli, M. Huang, R. K. Batra, and S. M. Dubinett. 2005. Tumor cyclooxygenase-2/prostaglandin E$_2$-dependent promotion of FOXP3 expression and CD4$^+$ CD25$^+$ T regulatory cell activities in lung cancer. *Cancer Res.* 65: 5211–5220.
43. Toossi, Z., J. R. Sedor, J. P. Lapurga, R. J. Ondash, and J. J. Ellner. 1990. Expression of functional interleukin 2 receptors by peripheral blood monocytes from patients with active pulmonary tuberculosis. *J. Clin. Invest.* 85: 1777–1784.
44. Barral-Netto, M., A. Barral, S. B. Santos, E. M. Carvalho, R. Badaro, H. Rocha, S. G. Reed, and W. D. Johnson, Jr. 1991. Soluble IL-2 receptor as an agent of serum-mediated suppression in human visceral leishmaniasis. *J. Immunol.* 147: 281–284.
45. Makis, A. C., E. Galanakis, E. C. Hatzimichael, Z. L. Papadopoulou, A. Siamopoulou, and K. L. Bourantas. 2005. Serum levels of soluble interleukin-2 receptor alpha (sIL-2Rα) as a predictor of outcome in brucellosis. *J. Infect.* 51: 206–210.
46. Sheibani, K., C. D. Winberg, S. van de Velde, D. W. Blayney, and H. Rappaport. 1987. Distribution of lymphocytes with interleukin-2 receptors (TAC antigens) in reactive lymphoproliferative processes. Hodgkin's disease, and non-Hodgkin's lymphomas: an immunohistologic study of 300 cases. *Am. J. Pathol.* 127: 27–37.
47. Janik, J. E., J. C. Morris, S. Pittaluga, K. McDonald, M. Raffeld, E. S. Jaffe, N. Grant, M. Gutierrez, T. A. Waldmann, and W. H. Wilson. 2004. Elevated serum-soluble interleukin-2 receptor levels in patients with anaplastic large cell lymphoma. *Blood* 104: 3355–3357.
48. Herbert, K. C., and S. J. Foster. 2001. Starvation survival in *Listeria monocytogenes*: characterization of the response and the role of known and novel components. *Microbiology* 147: 2275–2284.
49. Marquis, H., H. G. Bouwer, D. J. Hinrichs, and D. A. Portnoy. 1993. Intracytoplasmic growth and virulence of *Listeria monocytogenes* auxotrophic mutants. *Infect. Immun.* 61: 3756–3760.
50. Gutierrez-Preciado, A., R. A. Jensen, C. Yanofsky, and E. Merino. 2005. New insights into regulation of the tryptophan biosynthetic operon in Gram-positive bacteria. *Trends Genet.* 21: 432–436.
51. Kaufmann, S. H. 1993. Immunity to intracellular bacteria. *Annu. Rev. Immunol.* 11: 129–163.
52. Tufariello, J. M., J. Chan, and J. L. Flynn. 2003. Latent tuberculosis: mechanisms of host and bacillus that contribute to persistent infection. *Lancet Infect. Dis.* 3: 578–590.
53. Kindler, V., A. P. Sappino, G. E. Grau, P. F. Piguet, and P. Vassalli. 1989. The inducing role of tumor necrosis factor in the development of bactericidal granulomas during BCG infection. *Cell* 56: 731–740.
54. Ehlers, S., C. Holscher, S. Scheu, C. Tertilt, T. Hehlgans, J. Suwinski, R. Endres, and K. Pfeffer. 2003. The lymphotoxin β receptor is critically involved in controlling infections with the intracellular pathogens *Mycobacterium tuberculosis* and *Listeria monocytogenes*. *J. Immunol.* 170: 5210–5218.
55. Kuuliala, A., R. Nissinen, H. Kautiainen, H. Repo, and M. Leirisalo-Repo. 2006. Low circulating soluble interleukin 2 receptor level predicts rapid response in patients with refractory rheumatoid arthritis treated with infliximab. *Ann. Rheum. Dis.* 65: 26–29.
56. Wolf, A. M., D. Wolf, H. Rumpold, A. R. Muschen, A. Kaser, P. Obrist, D. Fuchs, G. Brandacher, C. Winkler, K. Geboes, P. Rutgeerts, and H. Tilg. 2004. Overexpression of indoleamine 2,3-dioxygenase in human inflammatory bowel disease. *Clin. Immunol.* 113: 47–55.
57. Detkova, Z., V. Kupcova, M. Prikazska, L. Turecky, S. Weissova, and E. Jahnova. 2003. Different patterns of serum interleukin 10 response to treatment with anti-tumor necrosis factor α antibody (infliximab) in Crohn's disease. *Physiol. Res.* 52: 95–100.
58. Keane, J., S. Gershon, R. P. Wise, E. Mirabile-Levens, J. Kasznica, W. D. Schwieterman, J. N. Siegel, and M. M. Braun. 2001. Tuberculosis associated with infliximab, a tumor necrosis factor α-neutralizing agent. *N. Engl. J. Med.* 345: 1098–1104.
59. Slifman, N. R., S. K. Gershon, J. H. Lee, E. T. Edwards, and M. M. Braun. 2003. *Listeria monocytogenes* infection as a complication of treatment with tumor necrosis factor α-neutralizing agents. *Arthritis Rheum.* 48: 319–324.

Available online at www.sciencedirect.com

ScienceDirect

Immunology Letters 116 (2008) 95–102

Immunology Letters

www.elsevier.com/locate/

High-affinity uptake of kynurenine and nitric oxide-mediated inhibition of indoleamine 2,3-dioxygenase in bone marrow-derived myeloid dendritic cells

Toshiaki Hara [a], Nanako Ogasawara [a], Hidetoshi Akimoto [b], Osamu Takikawa [b], Rie Hiramatsu [a], Tsutomu Kawabe [a], Ken-ichi Isobe [c], Fumihiko Nagase [a,*]

[a] *Department of Medical Technology, Nagoya University School of Health Sciences, 1-20 Daikominami-1-chome, Higashi-ku, Nagoya, Aichi, 461-8673, Japan*

[b] *Institute of Longevity Science, National Center for Geriatrics and Gerontology, Obu, Aichi, Japan*

[c] *Department of Immunology, Nagoya University Graduate School of Medicine, Nagoya, Aichi, Japan*

Received 22 March 2007; received in revised form 14 November 2007; accepted 27 November 2007
Available online 26 December 2007

Abstract

Indoleamine 2,3-dioxygenase (IDO)-initiated tryptophan metabolism along the kynurenine (Kyn) pathway in some dendritic cells (DC) such as plasmacytoid DC (pDC) regulates T-cell responses. It is unclear whether bone marrow-derived myeloid DC (BMDC) express functional IDO. The IDO expression was examined in $CD11c^+CD11b^+$ BMDC differentiated from mouse bone marrow cells using GM-CSF. CpG oligodeoxynucleotides (CpG) induced the expression of IDO protein with the production of nitric oxide (NO) in BMDC in cultures for 24 h. In the enzyme assay using cellular extracts of BMDC, the IDO activity of BMDC stimulated with CpG was enhanced by the addition of a NO synthase (NOS) inhibitor, suggesting that IDO activity was suppressed by NO production. On the other hand, the concentration of Kyn in the culture supernatant of BMDC was not increased by stimulation with CpG. Exogenously added Kyn was taken up by BMDC independently of CpG stimulation and NO production, and the uptake of Kyn was inhibited by a transport system L-specific inhibitor or high concentrations of tryptophan. The uptake of tryptophan by BMDC was markedly lower than that of Kyn. In conclusion, IDO activity in BMDC is down-regulated by NO production, whereas BMDC strongly take up exogenous Kyn.

Keywords: Bone marrow-derived myeloid dendritic cells; Indoleamine 2,3-dioxygenase; Tryptophan; Kynurenine; Nitric oxide; Transport system L

1. Introduction

Indoleamine 2,3-dioxygenase (IDO)-initiated tryptophan (Trp) metabolism along the kynurenine (Kyn) pathway regulates T-cell responses in some dendritic cells (DC) such as plasmacytoid DC (pDC) or $CD8^+$ DC in mouse spleen cells [1,2]. Two mechanisms of IDO to inhibit T-cell responses are proposed; the local depletion of Trp required for cell proliferation and the induction of apoptosis or growth arrest by Trp metabolites [1]. Three functionally distinct subsets of DC are defined in mouse spleen cells and include the plasmacytoid DC, $CD8^+$ and $CD8^-$ conventional DC (cDC) [3]. DC generated in culture from mouse bone marrow precursors with GM-CSF [4] or GM-CSF and IL-4 are mainly $CD11c^+CD11b^+$ myeloid DC, whereas cell culture from mouse bone marrow cells with Fms-like tyrosine kinase 3 ligand (Flt3-L) allows the generation of both cDC and pDC [5–7]. Human myeloid DC differentiated from blood monocytes with GM-CSF and IL-4 or macrophages differentiated with M-CSF express functionally active IDO [8,9]. It has recently been shown that thymosin α1 activates IDO in GM-CSF/IL-4- or Flt3-L-developed DC from mouse bone marrow cells [10].

IDO is induced by inflammation or immune responses such as infectious or tumor immunity. IDO expression is induced in DC by various stimuli such as IFN-γ, toll-like receptor (TLR)-ligation by LPS or CpG oligodeoxynucleotides (CpG) or CD80/CD86-ligation by CTLA-4 expressed on the regulatory T cells [1]. CpG, which is a strong immune stimulator, also possesses immune suppressive activity through the induction of

* Corresponding author. Tel.: +81 52 719 1189; fax: +81 52 719 1189.
E-mail address: nagase@met.nagoya-u.ac.jp (F. Nagase).

0165-2478/$ – see front matter © 2007 Elsevier B.V. All rights reserved.
doi:10.1016/j.imlet.2007.11.016

IDO [11–14]. TLR-9 signaling from CpG activates NF-κB and p38 through MyD88 and IRF-8 in DC [15]. CpG is the TLR ligand to induce IDO mRNA in bone marrow-derived myeloid DC (BMDC) [12].

IDO protein can be expressed without functional enzymatic activity. Isolated mouse splenic $CD8^+$ DC were found to catabolize Trp when exposed to IFN-γ, whereas other $CD8^-$ DC did not, even though both subsets expressed comparable amounts of IDO protein as analyzed by Western blot [16]. It is not yet clear why IDO protein expressed in $CD8^-$ DC is not functional.

IDO activity of IFN-γ-activated murine peritoneal macrophages was induced by inhibition of nitric oxide synthase (NOS) [17]. Incorporation of the heme prosthetic group into active site is required for IDO activity, and inhibition of IDO activity by NO generators was abrogated by co-addition of oxyhemoglobin, an antagonist of NO function [17]. Both blocking of a heme site to O_2 binding and conformational changes induced by breaking the Fe–N bond have been proposed as important mechanisms by which NO inhibits IDO [18]. NO led to an accelerated degradation of IDO protein in the proteasome [19]. In addition, a peroxynitrite generator also inhibited IDO activity through the nitration of the selective tyrosines of IDO [20]. NO production was induced in BMDC by stimulation with IFN-γ and LPS [21].

It has recently been published that BMDC expressing IDO upon IFN-γ stimulation suppress OVA-specific $CD8^+$ T-cell proliferation [22,23]. However, these results are not consistent with the published report that IFN-γ enhances antigen-presenting activity in BMDC [24]. In the present study, we examined the functional expression of IDO in BMDC stimulated with CpG. BMDC expressed IDO protein upon CpG stimulation but its activity was inhibited by NO production. BMDC did not secrete Kyn upon CpG stimulation but took up exogenous Kyn.

2. Materials and methods

2.1. Reagents

The Phosphorothioate CpG1826 (5′-TCC ATG ACG TTC CTG ACG TT-3′), N^G-monomethyl-L-arginine acetate salt (NMA), L-Kyn, L-Trp, 2-amino-2-norbornanecarboxylic acid (BCH) and 1-methyl-DL-tryptophan (1-MT) were purchased from Sigma–Aldrich (St. Louis, MO). PE-conjugated anti-mouse CD11c and FITC-conjugated anti-mouse CD11b antibodies were purchased from eBioscience (San Diego, CA). Anti-mouse IDO polyclonal antibody was prepared as described previously [25]. Anti-inducible NOS (iNOS) polyclonal antibody was purchased from BD Bioscience (San Diego, CA).

2.2. Preparation of BMDC

C57BL/6 mice were purchased from Japan SLC (Shizuoka, Japan). BMDC were generated as described previously [4]. Briefly, bone marrow cells were cultured in RPMI1640 medium (10% fetal calf serum, 300 μg/ml glutamine, 100 U/ml penicillin, 100 μg/ml streptomycin and 50 μM 2-mercaptoethanol) containing 0.3% GM-CSF supernatant (from murine GM-CSF producing Chinese hamster ovary cells, a gift from T. Sudo, Toray Silicon, Tokyo, Japan). The DC culture medium was changed every 2 days to remove nonadherent cells. Loosely adherent clustering cells were collected on day 6 and used as immature DC. BMDC were activated by stimulation with CpG (5 μg/ml) alone or together with NMA (100 μM) for 24 h.

2.3. Flow cytometry

For detection of cell surface markers, cells were incubated with PE-conjugated anti-CD11c and FITC-conjugated anti-CD11b antibodies at 4 °C for 30 min. These cells were analyzed by an EPICS XL flow cytometer (Beckman Coulter).

2.4. Western blot

Western blot was carried out as described previously [26]. BMDC were stimulated with CpG (5 μg/ml) with or without NMA (100 μM) for 24 h. Then, cells were washed and lysed with 1× sample buffer and boiled for 3 min. The cell lysates were passed though a syringe with a 26G needle before being applied on 10% sodium dodecyl sulfate (SDS)-polyacrylamide gels. After electrophoresis, protein was transferred to a nitrocellulose membrane and the membrane was blocked with PBS plus 0.05% Tween 20 (PBST) containing 0.3% skimmed milk for 1 h at room temperature. Then the membrane was incubated with anti-IDO, anti-iNOS or anti-actin antibody at 4 °C overnight. The membrane was then washed with PBST and incubated with horseradish peroxidase-conjugated anti-rabbit IgG for 1 h at room temperature. Finally, the membrane was washed with PBST and developed with a Western lightning chemiluminescence reagent (PerkinElmer Life Sciences, Boston, MA).

2.5. Assay of NO production

The amount of NO production in the medium was estimated by the assay of nitrite using Griess reagent [27]. Fifty microliters of each supernatant was mixed with an equal volume of Griess reagent (1% sulfanilamide in 5% phosphoric acid and 0.1% naphthylethylenediamine dihydrochloride in distilled water). The absorbance of the mixture at 590 nm was determined by a plate reader, and the nitrite concentration was determined using standard solutions of sodium nitrite.

2.6. Enzyme assay of IDO activity

IDO activity was determined by the assay previously described [28]. After cells were sonicated, the homogenate was centrifuged at 10,000 rpm for 10 min. The supernatant (100 μl) was mixed with an equal volume of 2× reaction buffer (100 mM potassium phosphate buffer pH 6.5, 40 mM sodium ascorbate, 20 μM methylene blue, 200 μg/ml catalase, and 800 μM Trp). The mixtures were incubated at 37 °C for 60 min to permit IDO to convert Trp to *N*-formylkynurenine, and then 40 μl of 30% (w/v) TCA was added to stop the

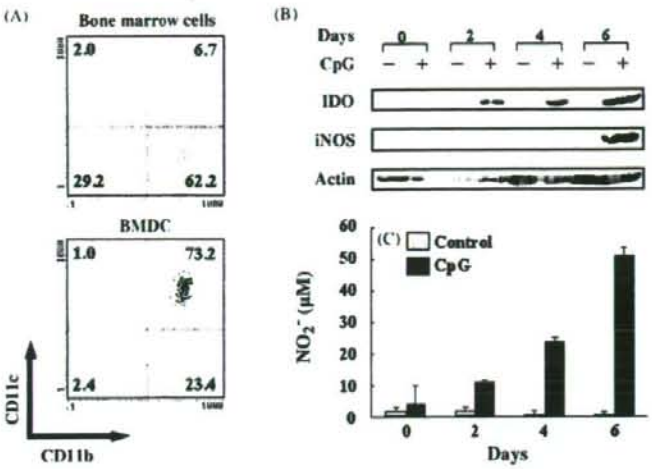

Fig. 1. The induction of IDO expression and NO production in BMDC stimulated with CpG. (A) Surface expression of CD11c and CD11b on bone marrow cells or BMDC was analyzed by flow cytometry. The percentage of cells in each quadrant is presented. (B and C) Cells (10^6 cells/ml) collected after cultures of bone marrow cells for the indicated days were stimulated with CpG for 24 h. (B) IDO and iNOS expressions were assessed by Western blot. (C) Nitrite accumulation in the culture supernatant was measured using Griess reagent. Means ± S.D. of triplicate cultures are presented.

reaction. After heating at 50 °C for 30 min, the reaction mixtures were centrifuged and Kyn concentration in the supernatant was measured by high-pressure liquid chromatography (HPLC).

2.7. Assay of Kyn and Trp

Concentrations of Kyn and Trp were determined by HPLC as previously described [28], with minor modification. Before HPLC assay, culture medium was deproteinized by treatment with 86% methanol (1:6, v/v). Twenty-five microliters of sample was injected into a 5 μm endcapped Purospher RP-18 column (Merck, Darmstadt, Germany) and analyses were carried out at a flow rate of 1.0 ml/min. The mobile phase was 10 mM acetic ammonium (pH 6.5) and 10% methanol. Kyn was detected by a UV-detector at a wavelength of 360 nm and Trp by a fluorescence detector at an excitation wavelength of 285 nm and an emission wavelength of 365 nm.

2.8. Assay of Kyn uptake

For the assay of Kyn uptake for a short time, BMDC were washed with Tris–choline buffer (150 mM choline chloride, 10 mM Tris, pH 7.4) and suspended at 3×10^5 cells/0.2 ml per well in Tris–choline buffer or Tris–Na buffer (150 mM sodium chloride, 10 mM Tris, pH 7.4). Kyn was added into cell suspensions with or without BCH, Trp, or 1-MT in water bath at 37 °C. Kyn uptake was stopped by cooling cell suspension on ice. Kyn concentrations of the culture supernatant were assayed by HPLC, and the decrease of Kyn

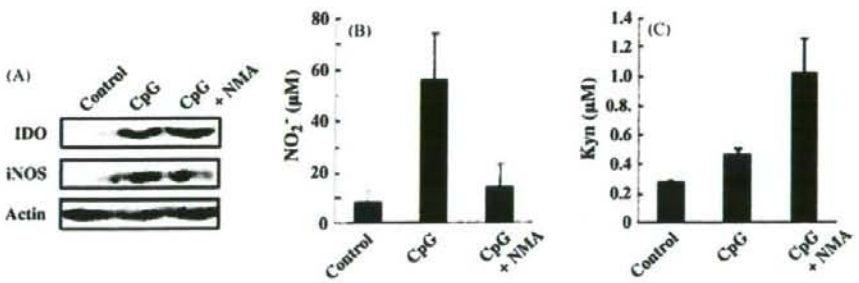

Fig. 2. The inhibition of IDO activity by NO production in BMDC stimulated with CpG. BMDC (10^6 cells/ml) were stimulated with CpG alone or together with NMA for 24 h. (A) The expression of IDO and iNOS proteins was assessed by Western blot. (B) Nitrite accumulation in the culture supernatant was measured using Griess reagent. (C) IDO activity was determined via Kyn formation using cellular extract as described under Section 2. (B and C) Means ± S.D. of triplicate cultures are presented.

content in the supernatant was estimated as Kyn uptake by BMDC.

3. Results

3.1. Expression of IDO protein and NO production in $CD11c^+CD11b^+$ BMDC by stimulation with CpG

BMDC were differentiated from bone marrow cells with GM-CSF for 6 days. Most (73.2%) of the BMDC were $CD11c^+CD11b^+$ myeloid DC (Fig. 1A). The expression of IDO and iNOS proteins was induced in BMDC but not original bone marrow cells stimulated with CpG for 24 h (Fig. 1B). CpG-mediated NO production was also increased with the BMDC development (Fig. 1C). These results indicate that the ability of BMDC to express IDO and iNOS proteins upon CpG stimulation is induced in the fully developed BMDC.

3.2. Inhibition of IDO activity by NO production in BMDC

Effects of NO production on IDO activity in BMDC were tested. IDO protein was expressed in BMDC by stimulation with CpG in the presence or absence of NMA, a NOS inhibitor (Fig. 2A). CpG-mediated NO production was inhibited by NMA (Fig. 2B). In the enzyme assay using cellular extracts of BMDC, IDO activity of BMDC stimulated with CpG was weak but enhanced by the addition of NMA (Fig. 2C). These results show that expression of IDO protein is induced in BMDC stimulated with CpG, although its activity is inhibited by NO production.

3.3. Non-secretion of Kyn by BMDC stimulated with CpG

We examined whether BMDC secreted Kyn upon stimulation with CpG. The Kyn level in the culture supernatant of BMDC was not increased significantly by stimulation with CpG even in the presence of exogenously added Trp (Fig. 3A). Correspondingly, the concentration of Trp in the culture supernatant of BMDC stimulated with CpG was hardly decreased unless NMA was added (Fig. 3B). These results indicate that BMDC do not secrete Kyn upon CpG stimulation.

3.4. Uptake of exogenously added Kyn by BMDC without CpG stimulation

It has been recently shown that $CD8^-$ DC takes up exogenously added Kyn upon IFN-γ stimulation [29]. Therefore, we examined whether exogenously added Kyn was taken up by BMDC by CpG stimulation for 24 h. The Kyn concentration in the culture supernatant of BMDC was decreased by around 20% independently of CpG stimulation and NMA when 50 μM Kyn was exogenously added (Fig. 4A). The Kyn concentration in the culture supernatant of BMDC was decreased dependently on the concentration of exogenously added Kyn (10–100 μM) (Fig. 4B). Concentrations of Kyn in the culture supernatants of BMDC were decreased almost linearly with time for 24 h (Fig. 4C). The ability of BMDC to take up Kyn was induced with the development from bone marrow cells (Fig. 4D). These results suggest that BMDC take up Kyn independently of IDO expression and NO production.

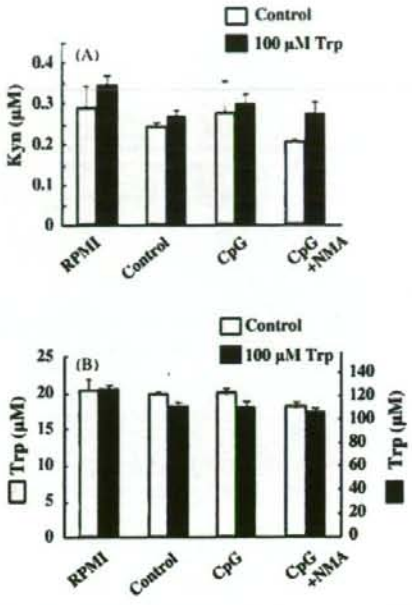

Fig. 3. The non-secretion of Kyn by BMDC stimulated with CpG. BMDC (3×10^5 cells/0.2 ml) were stimulated with CpG alone or together with NMA in the presence or absence of exogenously added Trp (100 μM) for 24 h. Concentrations of (A) Kyn or (B) Trp in the culture supernatant of BMDC were measured by HPLC. Means ± S.D. of triplicate cultures are presented.

3.5. Inhibition of Kyn uptake by a transport system L-specific inhibitor and Trp

It has been shown that astrocytes take up Kyn through a Na^+-independent transport system L [30]. Na^+-dependency of Kyn uptake by BMDC was tested in cultures of BMDC by using Na^+ and Na^+-free buffers for a short time. Kyn uptake by BMDC in Na^+-free buffer for 15 min was higher than that in Na^+ buffer (Fig. 5A), indicating that Kyn uptake by BMDC is mainly Na^+-independent. Therefore, Kyn uptake by BMDC was tested in Na^+-free buffer. The uptake of exogenously added Kyn (10 μM) by BMDC (3×10^5 cells) increased rapidly to around 100 pmol (5% of Kyn exogenously added) within 2 min and gradually thereafter (Fig. 5B). Effects of the addition of Trp, BCH, a specific inhibitor of the transport system L, or 1-MT, an inhibitor of IDO and the transport system L [31–33], on Kyn uptake by BMDC were tested (Fig. 5C). All the BCH, Trp and 1-MT prevented the uptake of exogenously added Kyn by BMDC. These results show that Kyn is taken up by BMDC mainly through the transport system L.

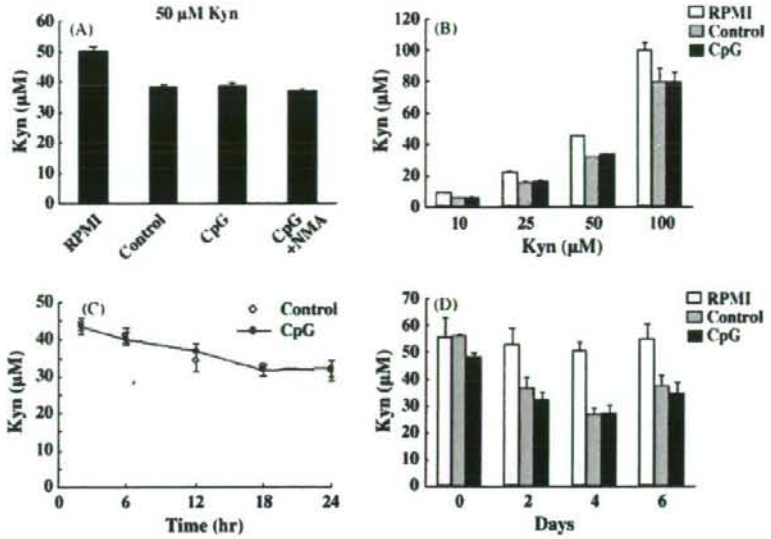

Fig. 4. Kyn uptake by BMDC independent of stimulation with CpG. (A–C) BMDC (3×10^5 cells/0.2 ml) or (D) cells collected after cultures of bone marrow cells for the indicated days were stimulated with CpG alone or together with NMA in the presence of exogenously added (A, C, and D) 50 μM or (B) the indicated concentration of Kyn for (A, B, and D) 24 h or (C) the indicated time (2–24 h). Concentrations of Kyn in the culture supernatant were measured by HPLC. Means ± S.D. of triplicate cultures are presented.

4. Discussion

The present study shows that the expression of IDO activity in BMDC is regulated at the post-transcriptional level by NO production. IDO activity of BMDC was detected only by the enzyme assay using the cellular extracts of BMDC stimulated with CpG in the presence of a NOS inhibitor. IFN-γ-activated mouse peritoneal macrophages secrete Kyn in the presence of a NOS inhibitor [17]. However, CpG-activated BMDC did not secrete Kyn even in the presence of a NOS inhibitor. This may be caused by the weak activity of IDO in BMDC. Human myeloid DC differentiated from blood monocytes with GM-CSF and IL-4 as well as macrophages differentiated with M-CSF express IDO activity [8,9]. These differences are caused by a clear species specificity regarding the induction of IDO versus iNOS in cultured cells [34]. In human monocytes/macrophages, IFN-γ or IFN-γ/LPS strongly induces IDO, but not iNOS activity, while in mouse macrophages these stimuli strongly induce iNOS, but not IDO activity. Thus, the inhibition of iNOS expression is at least required for the induction of IDO activity.

We showed the expression of IDO protein, non-secretion of Kyn and NO production in BMDC stimulated with CpG. IFN-γ-activated $CD8^-$ DC in mouse spleen express IDO protein but not IDO activity in contrast to $CD8^+$ DC [16]. $CD8^-$ DC treated with IFN-γ produce significantly higher levels of NO than the $CD8^+$ DC counterpart [16]. Thus, activated myeloid dendritic cells such as BMDC and $CD8^-$ DC express IDO protein and produce NO but do not secrete Kyn. Unexpectedly, Park and coworkers have recently published that IDO-expressing BMDC upon IFN-γ stimulation suppress OVA-specific $CD8^+$ T-cell proliferation [22,23]. However, IFN-γ induces high levels of NO production [21], and enhances antigen-presenting activity in BMDC [24]. At present, it is difficult to reconcile these observations [22,23] with our finding that the activity of IDO is suppressed by NO production in BMDC stimulated with CpG and also with the enhancement of antigen-presenting activity of BMDC stimulated with IFN-γ [24].

Bone marrow cells neither expressed IDO and iNOS proteins nor produced NO upon CpG stimulation without differentiation to BMDC with GM-CSF (Fig. 1B and C). GM-CSF induces NO production in a skin dendritic cell line and enhances IDO expression in eosinophils stimulated with IFN-γ [35,36]. Thus, GM-CSF seems to be an important factor for the induction of IDO and iNOS. However, GM-CSF completely inhibits Flt3-L-induced pDC development from bone marrow cells [5,6]. As far as we know, there is no report showing that high levels of NO production are induced in pDC. Therefore, GM-CSF seems to be a much more critical factor in vitro for the induction of iNOS than that of IDO with BMDC differentiation.

The development of $CD8^-$ DC from bone marrow cells in the presence of GM-CSF depends on IRF-4, whereas the development of $CD8^+$ DC and pDC in the presence of Flt3-L mainly depends on IRF-8 [37,38]. Correspondingly, the negative regulation of gene expression of IRF-8 inhibits the induction of IDO activity in $CD8^+$ DC or LPS-matured human DC stimulated with IFN-γ [39]. Induction of IDO by LPS but not IFN-γ in human monocytic THP-1 cells involves p38 and NF-κB pathways [40]. TLR-9 signaling from CpG activates p38 and NF-κB through MyD88 and IRF-8 in DC [15]. BMDC developed from bone marrow cells with GM-CSF express significantly IRF-8 [37,38]. Therefore, it may be possible that BMDC express IDO protein through MyD88 and IRF-8 in response to CpG. However,

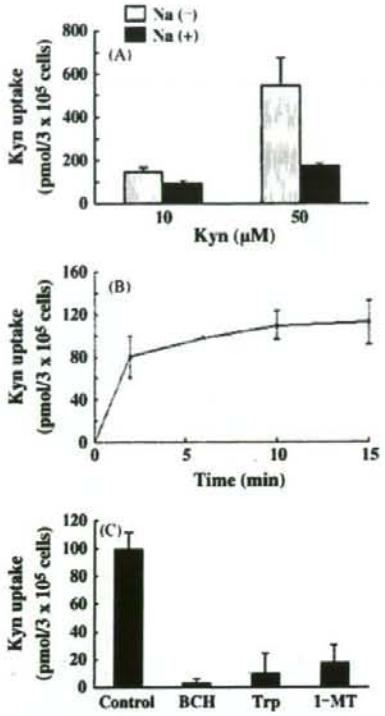

Fig. 5. Kyn uptake by BMDC through transport system L. (A) BMDC (3×10^5 cells/0.2 ml) were incubated with Kyn (10 or 50 μM) in Tris–choline buffer or Tris–Na buffer for 15 min. (B and C) BMDC (3×10^5 cells/0.2 ml) were incubated with 10 μM Kyn in (B) Tris–choline buffer for 0–15 min or (C) together with 2 mM BCH, Trp or 400 μM 1-MT for 15 min. Concentrations of Kyn in the culture supernatant were measured by HPLC. Means ± S.D. of triplicate cultures are presented.

it has recently been shown that LPS but not IFN-γ induces the IDO expression in BMDC through the activation of PI3 kinase and JNK [41]. Therefore, it is interesting to clarify which signal pathways are required for the induction of IDO in BMDC by stimulation with CpG.

We showed that BMDC took up exogenous Kyn independently of CpG stimulation and NO production. Na^+-independent uptake of Kyn by BMDC was blocked by BCH, a transport system L-specific inhibitor, Trp or 1-MT blocked. The transport of Kyn in BMDC is similar to that in astrocytes, which is inhibited by BCH and Trp in Na^+-free solution [30]. BCH, Trp, 1-MT and various other amino acids also inhibit Trp uptake through the transport system L [31–33]. A BCH-sensitive and Na^+-independent transport is consistent with system L, a neutral amino acid transport mechanism, being the major conduit of Trp [31–33]. Therefore, we conclude that BMDC take up Kyn mainly through the transport system L.

We showed that BMDC took up Kyn much more preferentially than Trp, indicating a higher affinity of Kyn than Trp to the transporter. A low affinity of Trp to the transporter corresponds to the expression of a low IDO activity in BMDC. In fact, the enzyme assay of IDO activity using the cellular extract of BMDC, which does not require membrane transport of Trp, demonstrated IDO activity. A high-affinity, Trp-selective amino acid transport system has been recently shown in human macrophages, and speculated that this unique transport system allows macrophages to take up Trp efficiently under low substrate concentration, such as may occur during interaction between T cells and IDO-expressing antigen-presenting cells [42]. Taken together with our findings, a low affinity of Trp to the transporter in BMDC causes the expression of a low IDO activity, in addition to the suppression by NO production.

It has recently been shown that $CD8^-$ DC as well as $CD8^+$ DC take up exogenously added Kyn and secrete quinolinic acid upon IFN-γ stimulation [29]. Therefore, DC such as BMDC, $CD8^-$ DC and $CD8^+$ DC take up exogenous Kyn. However, the uptake of Kyn by BMDC is independent of CpG stimulation. Therefore, it is suggested that CpG does not activate down stream enzymes of IDO along the Kyn pathway. On the other hand, immunogenic $CD8^-$ DC became immunosuppressive DC through the generation of Kyn metabolites such as quinolinic acid upon IFN-γ stimulation in the presence of exogenous Kyn [29]. However, we did not observe the immunosuppressive activity of BMDC stimulated with IFN-γ in the presence of exogenously added Kyn (unpublished data). Our results suggest a new possibility that BMDC counteracts Kyn-mediated induction of regulatory DC or T cells by scavenging Kyn.

The utilization of Kyn by BMDC in the resting state might be physiologically important for cell survival because IDO is not constitutively activated. Moffett et al. have shown that intraperitoneal injections of Kyn did not result in any significant increase in hepatocyte immunoreactivity with quinolinate-specific antibody, but rather led to dramatic increase in immunoreactivity in tissue macrophages, splenic white pulp, and thymic medulla [43,44]. Quinolinic acid formation was also induced most strongly in spleen by systemic immune stimulation with pokeweed mitogen [45]. Therefore, it is suggested that extrahepatic Kyn is preferentially metabolized in immune cells involving BMDC. It may be possible that Kyn is utilized for NAD synthesis for the survival of BMDC as shown in RAW264.7 macrophages [46]. Trp metabolism along the Kyn pathway is also required for DC activation [47]. Further study is required in order to clarify the fate of Kyn taken up by BMDC.

GM-CSF induces in vivo as well as in vitro the development of myeloid DC, whereas Flt3-L induces the development of both myeloid DC and pDC [5–7,48,49]. Thus, the activity of GM-CSF to induce in vitro the development of immunogenic myeloid DC from bone marrow cells correlates with the physiological activity of GM-CSF in vivo. In interaction between DC subsets, otherwise immunogenic $CD8^-$ DC become tolerogenic in co-culture with $CD8^+$ DC upon IFN-γ stimulation [29]. The present study suggests alternative possibility that myeloid DC differentiated with GM-CSF up-regulates immune responses by counteracting tolerogenic activity of IDO-expressing DC through the two independent mechanisms; the inhibition of IDO activity by NO production and scavenging Kyn secreted from tolerogenic DC.